Scattering by a Perfectly Conducting Multi-Slotted Circular Cylinder

by

Mousa Issa M. Hussein

A thesis

presented to the University of Manitoba

in fulfilment of the

thesis requirement for the degree of

Master of Science

in

Electrical and Computer Engineering

Winnipeg, Manitoba, Canada 1991

ISBN 0-315-77991-8

SCATTERING BY A PERFECTLY CONDUCTING MULTI-SLOTTED CIRCULAR CYLINDER

BY

MOUSA ISSA M. HUSSEIN

A thesis submitted to the Faculty of Graduate Studies of the University of Manitoba in partial fulfillment of the requirements of the degree of

MASTER OF SCIENCE

I hereby declare that I am the sole author of this thesis.

I authorize the University of Manitoba to lend this thesis to other institutions or individuals for the purpose of scholarly research.

I further authorize the University of Manitoba to reproduce this thesis by photocopying or by other means, in total or in part, at the request of other institutions or individuals for the purpose of scholarly research.

ABSTRACT

The problem of scattering by a perfectly conducting multi-slotted circular cylinder excited by a z-polarized TM incident plane wave is presented. The solution is carried out using two methods of analysis. In the first method the problem is analyzed using the boundary value method. Field components inside and outside the cylinder are obtained in terms of the aperture fields. Then Galerkin's method is employed to solve for the unknown aperture fields. In the second method the unknown aperture fields are obtained using the aperture field integral equation method. Upon application of the boundary condition, N-integral equations are obtained. The resulting integral equations are solved using the method of moments. Results for the surface tangential electric electric fields, the far scattered field and the bistatic scattering width are obtained and compared using the two proposed methods.

ACKNOWLEDGEMENTS

I would like to express my sincere gratitude to Professor M. Hamid for his advice, continuous encouragement and helpful discussion and advice throughout the course of this research. I would also like to thank my committee members, Professor A. Sebak and Professor J. Cahoon, for their valuable comments and advice.

Special thanks to my wife and daughter Huda for their patience and continuous encouragement and to my parents for their valuable support and encouragement across the Atlantic.

Finally, I would like to acknowledge the financial assistance of the Natural Science and Engineering Research Council of Canada and the Faculty of Graduate studies of the University of Manitoba, which made this research possible.

TABLE OF CONTENTS

LIST OF FIGURES

FIGURE **PAGE**

FIGURE **PAGE**

LIST OF PRINCIPAL SYMBOLS

j	$\sqrt{-1}$
ϕ_i	angle of incidence field
k_o	free space wave number
k_1	dielectric media wave number
ε_n	Nueman number
ε_o	Permittivity of free space
μ_o	Permeability of free space
ε_1	Permittivity of dielectric material
μ_1	Permeability of dielectric material
J_n	Bessel function of order n
J_n'	derivative of Bessel function
$H_n^{(2)}$	Hankel function of second kind and order n
$H_n'^{(2)}$	derivative of Hankel function
A_n	transmitted field expansion coefficients
B_n	scattered field expansion coefficients
y_o	free space intrinsic impedance
y_1	dielectric media intrinsic impedance
a_q	aperture field expansion coefficients
$E(\phi)$	aperture field

M_q	aperture vector basis functions
$\delta(x)$	Dirac delta function
$\sigma(\phi)$	bistatic scattering width
ε_r	relative permitivitty
ka	cylinder electric radius
N	number of slots
a_{q_j}	the j^{th} aperture field expansion coefficients
$E_j(\phi)$	the j^{th} aperture field
M_{q_j}	the j^{th} aperture vector basis functions
b_{q_j}	aperture field expansion coefficients

CHAPTER 1

INTRODUCTION

The scattering of electromagnetic waves from an infinite axial, perfectly conducting circular cylinder with a single or multi-slot, situated in free space and excited by a plane wave or an electric/magnetic line source is a well known problem in electromagnetic field theory. Recently the circular slotted cylinder filled with a dielectric material has become the subject of extensive study due to its engineering applications in devices such as microstrip transmission lines, microstrip antennas and composite missiles.

This problem can be classified into two categories according to the excitation, i.e. the H-polarization transverse electric TE_z and E-polarization transverse magnetic TM_z waves. The H-polarization case has received a detailed treatment as an antenna problem [1]. Olte [2] studied the radiation of an elementary cylinder antenna through a slotted enclosure, where he reduced the problem to a Fredholm integral equation of the first kind, and then solved for a narrow slot as a special case. Richmond and Gilreath [3] studied a flush-mounted dielectric-loaded axial slot on a circular cylindrical antenna. The analysis was carried out using the boundary value method and then Galerkin's method was introduced to complete the solution. Simultaneous linear equations were generated in which the unknown quantities were

the coefficients in a Fourier series expansion for the electric field in the outer aperture. Johnson and Ziolkowski [4] used the generalized dual solution to solve for the scattering of an H-polarized plane wave from an axial slotted infinite cylinder. This solution was introduced by Ziolkowski [5] to solve the mixed boundary problem of the electromagnetic aperture coupling type. The diffraction problem for a narrow slot was treated by Rhodes [6] and by Morse and Feshback [7]. Beren [8] made a comparison study between three methods of solution. In one method, the aperture field integral equation method was used, while in the other two methods (E-field integral equation and H-field integral equation) the fields were determined from an equivelant surface current. Although the H-field integral equation method gives good results under some conditions, the solution becomes inaccurate under two other conditions which have to do with the interior resonance phenomenon [9] in which nonunique solutions are obtained. However, the other two methods were in a very good agreement and gave accurate results.

The E-polarization case has received some attention in the literature where various techniques were employed. It was investigated with an integral equation approach by Senior [10] and with approximate analytical approaches by Libelo [11]. Shestopalov et al. [12] have examined the problem with limiting cases of its dual series solution. Sinclair [13] has investigated the scattering from a perfectly conducting notched cylinder by using the reciprocity theorem, and his solution has been generalized to include other geometries such as the conducting cylindrical wedge, ribbon

and strip. Yatom [14] extended the solution of the conducting notched cylinder to the coated notched cylinder and the reciprocity theorem was used in conjunction with the boundary value method. The problem of a single slot was also studied in detail by Hussein [15]. Kishk [16] used the surface integral equation technique to characterize the electromagnetic scattering from a surface impedance three dimensional object partially coated with dielectric material. The resulting integral equations are solved for bodies of revolution using the method of moments.

The problem of a multi-slot conducting cylinder did not receive great deal of attention in the literature. Hussein [17] studied in detail the multi-slot problem. However the geometry was utilized in the same manner as other structures such as the coupling between waveguide in infinite arrays [18] and coupling between double step discontinuities in waveguide [19].

The main objective of this thesis is to present an analytical study of the fields in and around the cylinder for single and multi-slots with various values of slot parameters. The study is carried out using two methods of analysis. In the first method, the boundary value technique is employed, while in the second method the aperture field integral equation is used with the final computation carried out using the method of moments.

In Chapter 2 the case of a single slot with an arbitrary slot angle is considered. The cylinder is taken to be perfectly conducting, situated in free space, filled with a dielectric material, and excited by a z-polarized transverse magnetic TM_z plane

wave. The analysis is carried out using two methods as stated before. Both methods require the technique of separation of variables to start with [20], where the fields in and around the cylinder are found using Maxwell's equations. In the first method, the unknown aperture field is expressed in terms of a complete set of continuous and orthogonal functions defined on their respective domains. Application of the boundary conditions requires the use of the boundary value technique along with Galerkin's method. Simultaneous linear equations are generated in which the unknown quantities are the coefficients in a Fourier series expansion for the aperture electric field. In the second method, the unknown aperture field is expressed in terms of a discrete set of functions with unknown expansion coefficients defined only at discrete points on the aperture. The method of moments is used in conjunction with the aperture field integral equation technique to solve for the unknown expansion coefficients.

Chapter 3 presents the general solution for the case of a multi-slot cylinder. The cylinder is taken to be the same as the one specified in Chapter 2 except that it has N-arbitrary slots. The analysis used here is similar to the one used in Chapter 2, with the exception that there are N-coupled equations according to the number of slots. Moreover, the unknown aperture fields are expressed in terms of a continuous orthogonal functions, each defined in its respective domain. The boundary value technique requires the use of Galerkin's method N-times in order to generate N-coupled equations which contain the information on the aperture fields. Simi-

larly, there should be N-coupled aperture field integral equations which also contain the information that specifies the behavior of the aperture fields. The method of moments is then employed to solve the N-integral equations simultaneously.

Chapters 4 and 5 present numerical results for the single-slot case and the multi-slot case,respectivily. The results are classified into three parts. The first is used to examine the accuracy of the solution over the boundary region and to verify the validity of the solution for the complete conducting case. The second part discusses the results for the far scattered field with an arbitrary slots angle. The third part presents results and discussions for the bistatic scattering width. Conclusions and recommendations for future work are presented in Chapter 6.

CHAPTER 2

ANALYSIS OF SCATTERING BY A PERFECTLY CONDUCTING SINGLE-SLOTTED CIRCULAR CYLINDER

The problem of scattering by a perfectly conducting infinite cylinder with a single axial slot is presented in this chapter. Two methods of analysis are used to analyze the problem under consideration. Using Maxwell's equations and the technique of separation of variables, field components in and around the cylinder are found with unknown complex expansion coefficients. An unknown tangential electric field is assumed at the aperture. In the first method, application of the boundary conditions require continuity of the tangential electric field components in and around the cylinder with the aperture electric field. Continuity of the tangential magnetic field components across the aperture using the boundary value technique employs Galerkin's method, upon which the fields in and around the cylinder are found in terms of the aperture field. On the other hand, the second method employs the continuity of the tangential magnetic field components across the aperture to yield an integral equation in terms of the unknown aperture field. In order to solve this integral equation, the method of moments is employed [21]. The unknown

aperture field is expressed as an infinite series with a linear combination of the expansion function. The expansion function is substituted into the integral equation, then a weighting (testing) function is defined and used to test the integral equation at different points.

2.1 Boundary Value Method

The boundary value method is used to solve problems for which the field in a given region of space is determined from a knowledge of the field over the boundary of the region [20].

Consider a perfectly conducting circular cylinder of radius a, with an infinite axial slot along the z-axis of angular width $\phi = \beta - \alpha + 2\pi$. The inner region of the cylinder is assumed filled with dielectric material of permittivity ε_1 and permeability μ_1, and the outer region is taken to be free space. The cylinder is excited by a z-polarized transverse magnetic TM_z plane wave, with an incidence angle ϕ_i measured from the positive x-axis, as shown in Fig. 2.1. Since the source and the structure are independent of z, the field produced by this source can have only a z-component of the electric field that does not vary with z. Therefore, Maxwell's equations lead to the following tangintial wave equations.

$$(\nabla^2_{\rho,\phi} + k^2)E_z = 0 \tag{2.1}$$

and

$$H_\phi = \frac{1}{j\omega\mu}\frac{dE_z}{d\rho}. \tag{2.2}$$

where the time dependence $e^{j\omega t}$ is understood.

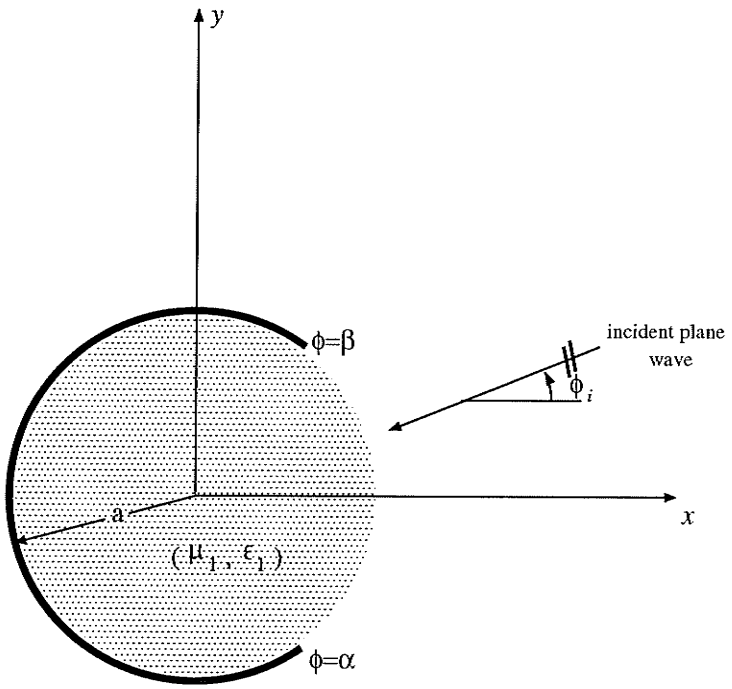

Figure 2.1: Geometry of the single slot problem.

The incident electric field of unit intensity due to a z-polarized plane wave is given by

$$E_z^i = e^{-jk\rho_o \cos(\phi-\phi_i)} \tag{2.3}$$

Using the wave transformation [20], (2.3) can be expanded in terms of cylindrical wave functions as

$$E_z^i = \sum_{n=0}^{\infty} j^n \varepsilon_n J_n(k_o\rho) \cos\, n(\phi - \phi_i) \tag{2.4}$$

The ϕ component of the incident field can be found using (2.2) to be

$$H_\phi^i = -jy_o \sum_{n=0}^{\infty} j^n \varepsilon_n J_n'(k_o\rho) \cos\, n(\phi - \phi_i) \tag{2.5}$$

Since the inner and outer regions of the cylinder are assumed to be continuous, smooth and of a circular geometry, the expressions for the total electric field components in both regions become

$$E_z^1 = \sum_{n=0}^{\infty} j^n \varepsilon_n A_n J_n(k_1\rho) \cos\, n\phi \qquad \rho < a \tag{2.6}$$

$$E_z^2 = \sum_{n=0}^{\infty} j^n \varepsilon_n \left[B_n H_n^{(2)}(k_o\rho) + J_n(k_o\rho)\right] \cos\, n(\phi - \phi_i) \qquad \rho > a\,. \tag{2.7}$$

The total ϕ components of the corresponding magnetic field can readily be found from (2.2)as

$$H_\phi^1 = -jy_1 \sum_{n=0}^{\infty} j^n \varepsilon_n A_n J_n'(k_1\rho) \cos\, n\phi \qquad \rho < a \tag{2.8}$$

$$H_\phi^2 = -jy_o \sum_{n=0}^{\infty} j^n \varepsilon_n \left[B_n H_n'^{(2)}(k_o\rho) + J_n'(k_o\rho)\right] \cos\, n(\phi - \phi_i) \qquad \rho > a\,. \tag{2.9}$$

Here J_n is the cylindrical Bessel function of order n, $H_n^{(2)}$ is the cylindrical Hankel function of the second kind and order n, the prime superscript denotes differentiation with respect to the total argument, y_o and y_1 are the intrinsic admittance of free space and dielectric material, respectively, while A_n are the unknown transmitted field coefficients and B_n are the unknown scattered field coefficients.

To solve for the unknown transmitting and scattering coefficients A_n and B_n, respectively, we have to satisfy the following boundary conditions:

$$E_z^1 = \begin{cases} E(\phi) & \alpha < \phi < \beta \\ 0 & \text{otherwise} \end{cases} \qquad \text{at} \quad \rho = a\,, \tag{2.10}$$

$$E_z^2 = \begin{cases} E(\phi) & \alpha < \phi < \beta \\ 0 & \text{otherwise} \end{cases} \qquad \text{at} \quad \rho = a\,, \tag{2.11}$$

and

$$H_\phi^1 = H_\phi^2 \qquad \text{at} \quad \rho = a \tag{2.12}$$

Continuity of the tangential electric fields can be accomplished by expanding the unknown aperture field $E(\phi)$ in terms of a complete set of orthogonal functions defined on their respective domains. The expansion function has to be of ϕ dependence only and z-directed. Also, it needs to be chosen to conform with the edge conditions at $\rho = a$, $\phi = \alpha$ and $\phi = \beta$. Moreover, the choice has to be appropriate and such that the integrals involved in the formulation are possible.

Therefore the continuity of the tangential electric field at $\rho = a$ gives

$$\sum_{n=0}^{\infty} j^n \varepsilon_n A_n J_n(k_1 a) \cos\, n\phi = \begin{cases} E(\phi) & \alpha < \phi < \beta \\ 0 & \text{otherwise} \end{cases}, \tag{2.13}$$

and

$$\sum_{n=0}^{\infty} j^n \varepsilon_n \left[B_n H_n^{(2)}(k_o a) + J_n(k_o a) \right] \cos\, n(\phi - \phi_i) = \begin{cases} E(\phi) & \alpha < \phi < \beta \\ 0 & \text{otherwise} \end{cases}. \tag{2.14}$$

$E(\phi)$ is the unknown aperture field and can be chosen as

$$E(\phi) = \sum_{q=1}^{\infty} a_q \sin \gamma(\phi - \alpha) \tag{2.15}$$

where $\gamma = \pi q/(\beta - \alpha)$ and $\beta \neq \alpha$.

Substituting back into (2.13) and (2.14) and making use of the orthogonality property of the trigonometric functions, the transmitting coefficients are be given by

$$A_n = \frac{j^{-n}}{\pi \varepsilon_n} \frac{1}{J_n(k_1 a)} \sum_{q=1}^{\infty} a_q \, F_{qn}\,, \tag{2.16}$$

where

$$F_{qn} = \int_{\alpha}^{\beta} \sin \gamma(\phi - \alpha) \cos\, n\phi \; d\phi\,. \tag{2.17}$$

and the scattered field coefficients become

$$B_n = \frac{1}{H_n^{(2)}(k_o a)} \left[\frac{j^{-n}}{\pi \varepsilon_n} \sum_{q=1}^{\infty} a_q G_{qn} - J_n(k_o a) \right], \tag{2.18}$$

where

$$G_{qn} = \int_{\alpha}^{\beta} \sin \gamma(\phi - \alpha) \cos\, n(\phi - \phi_i) \; d\phi\,. \tag{2.19}$$

The integrals in (2.17) and (2.19) can be evaluated analytically and can be written in closed forms.

Similarly, application of the continuity of the tangential magnetic field components gives

$$y_1 \sum_{n=0}^{\infty} j^n \varepsilon_n A_n J_n'(k_o a) \cos n\phi \;=\; y_o \sum_{n=0}^{\infty} j^n \varepsilon_n \left[B_n H_n'^{(2)}(k_o a) + J_n'(k_o a) \right] \cos n(\phi - \phi_i) \quad (2.20)$$

Substituting (2.16) and (2.18) into (2.20), and making use of the Wronskian determinant

$$J_n'(x) H_n'^{(2)}(x) - H_n'^{(2)}(x) J_n(x) = \frac{2j}{\pi x}\,, \quad (2.21)$$

one obtains

$$\sum_{q=1}^{\infty} a_q \sum_{n=0}^{\infty} \left[\frac{y_1}{y_o} \frac{J_n'(k_1 a)}{J_n(k_1 a)} F_{qn} \cos n\phi - \frac{H_n'^{(2)}(k_o a)}{H_n^{(2)}(k_o a)} G_{qn} \cos n(\phi - \phi_i) \right] = \frac{2j}{k_o a} \sum_{n=0}^{\infty} \frac{j^n \varepsilon_n}{H_n^{(2)}(k_o a)} \cos n(\phi - \phi_i) \quad (2.22)$$

In order for (2.22) to be evaluated for the unknown expansion coefficients a_q, Galerkin's technique has to be introduced, to enforce the continuity of the tangential magnetic field components across the aperture. Multiplying both sides of (2.22) by $\sin \gamma'(\phi - \alpha)$, where $\gamma' = \pi p/(\beta - \alpha)$, and integrating over the aperture, i.e. from $\phi = \alpha$ to $\phi = \beta$, the resulting equation can be written in a matrix form as follows.

$$[Z_{pq}]\ [a_q]\ = [V_p] \quad (2.23)$$

where

$$Z_{pq} = \sum_{n=0}^{\infty} \left[\frac{y_1}{y_o} \frac{J_n'(k_1 a)}{J_n(k_1 a)} F_{qn} F_{pn} - \frac{H_n'^{(2)}(k_o a)}{H_n^{(2)}(k_o a)} G_{qn} G_{pn} \right] \tag{2.24}$$

and

$$V_p = \frac{2j}{k_o a} \sum_{n=0}^{\infty} \frac{j^n \varepsilon_n}{H_n^{(2)}(k_o a)} G_{pn} \tag{2.25}$$

a_q in (2.23) represents the unknown field expansion coefficients

In matching H_ϕ across the aperture, a selection of the weighting function $\sin\gamma'(\phi - \alpha)$ was made to be the same as the basis function in (2.15). This is a distinctive feature of Galerkin's method.

The matrix equation in (2.23) can be solved to obtain numerical values for a_q, while (2.16) and (2.18) are employed to determine the unknown coefficients A_n and B_n, respectively.

2.2 Aperture Field Integral Equation

The same structure used in Section 2.1 will be used in this section to formulate the problem using the aperture field integral equation method. The electric and magnetic components in both regions will have the same expansion form as given by (2.6–2.9). Application of the boundary conditions (2.10–2.11), and making use of the orthogonality property of the trigonometric functions, the transmitting and scattering field coefficients can be obtained in an integral form as follows.

$$A_n = \frac{j^{-n}}{\pi \varepsilon_n} \frac{1}{J_n(k_1 a)} \int_\alpha^\beta E(\phi') \cos n\phi' d\phi', \tag{2.26}$$

$$B_n = \frac{1}{H_n^{(2)}(k_o a)} \left[\frac{j^{-n}}{\pi \varepsilon_n} \int_\alpha^\beta E(\phi') \cos n(\phi' - \phi_i)\, d\phi' - J_n(k_o a) \right]. \quad (2.27)$$

Now, making use of the remaining boundary condition given by (2.12), and substituting for A_n and B_n as given above by (2.26) and (2.27), respectively, one gets the following integral equation.

$$\sum_{n=0}^{\infty} \int_\alpha^\beta \left[\frac{y_1}{y_o} \frac{J_n'(k_1 a)}{J_n(k_1 a)} \cos n\phi \cos n\phi' - \frac{H_n'^{(2)}(k_o a)}{H_n^{(2)}(k_o a)} \cos n(\phi - \phi_i) \cos n(\phi' - \phi_i) \right] E(\phi')\, d\phi'$$
$$= \frac{2j}{k_o a} \sum_{n=0}^{\infty} \frac{j^n \varepsilon_n}{H_n^{(2)}(k_o a)} \cos n(\phi - \phi_i). \quad (2.28)$$

where ϕ' is a dummy variable of integration.

2.2.1 Method of Moments Algorithm

Equation(2.28) represents the aperture field integral equation, this equation is of a little use unless it can be evaluated analytically or can be computed numerically. Since the analytical approach has already been discussed in Section 2.1, the analysis will be carried out using a numerical technique. The method of moments [21] has proven to be one of the most efficient approximate method for obtaining results of acceptable accuracy. The results of the application of this approach to scattering problems is essentially a transformation of the original integral equation into a set of N linear equations in N unknowns. A linear combination of the N unknowns forms an approximation to the original unknown quantity appearing in the associated

integral equation. The above procedure may be written in a matrix equation of the following form

$$[\mathbf{Z}]\ [\mathbf{B}] = [\mathbf{V}]\ , \tag{2.29}$$

where $[\mathbf{Z}]$ is the coefficient matrix, $[\mathbf{B}]$ is the unknown quantity, and $[\mathbf{V}]$ is the known quantity of the matrix equation. The accuracy of the solution largely depends on the number of sampling points N and the approximate method used for evaluating the elements of the matrix $[\mathbf{Z}]$. However, since the determination of $[\mathbf{Z}]$ requires approximate evaluation of the sub-integral over N, better accuracy would require more accurate approximation techniques. Therefore, it seems advantageous to keep the number of sampling points, N, as low as possible and use more accurate techniques for evaluating $[\mathbf{Z}]$. Moreover, there is a limit on N beyond which the accuracy of the solution would greatly be impaired. Andreasen [22] has shown that for a smooth portion of the scatterer, the distance between two adjacent sampling points must not exceed $\lambda/4$. Furthermore, for regions close to the sharp edges, additional sampling points are needed.

2.2.2 Numerical Solution of the Integral Equation

To apply the method of moments to (2.28), the aperture field, $E(\phi)$ at $\rho = a$ and $\phi = \alpha$ to $\phi = \beta$, will be expanded in terms of basis functions and unknown

expansion coefficients as follows.

$$E(\phi) = \sum_{q=1}^{Q} b_q \, M_q \,, \tag{2.30}$$

where b_q are the unknown complex coefficients to be evaluated, and M_q are known basis functions. The above summation is limited to a finite number of terms Q. The choice of the basis functions, M_q, has no mathematical restrictions.

Equation (2.30) is substituted into (2.28) using pulse functions as basis functions. *i.e.*

$$M_q = \delta(\phi - \phi_q) = \begin{cases} 1 & \phi = \phi_q \\ 0 & \text{otherwise} \end{cases} \,. \tag{2.31}$$

A simple way to obtain an approximate solution is to require that equation (2.30) be satisfied at discrete points in the corresponding aperture. This procedure is called the point-matching method. Thus, selecting a set of testing functions, W_p, as

$$W_p = \delta(\phi - \phi_p) = \begin{cases} 1 & \phi = \phi_p \\ 0 & \text{otherwise} \end{cases} \,, \tag{2.32}$$

and defining an inner product as in [21]

$$< W, G > = \int_s W \cdot G \; ds \,, \tag{2.33}$$

where s is the aperture width. We see that equation (2.28) can finally be written in a matrix form as follows

$$\left[Z'_{pq}\right] \left[b_q\right] = \left[V'_p\right] \,, \tag{2.34}$$

where

$$Z'_{pq} = \sum_{n=0}^{\infty} \left[\frac{y_1}{y_o} \frac{J'_n(k_1 a)}{J_n(k_1 a)} \cos\, n\phi_q \cos\, n\phi_p - \frac{H'^{(2)}_n(k_o a)}{H^{(2)}_n(k_o a)} \cos\, n(\phi_q - \phi_i) \right.$$
$$\left. \cdot \cos\, n(\phi_p - \phi_i) \right] \qquad (2.35)$$

and

$$V'_p = \frac{2j}{k_o a} \sum_{n=0}^{\infty} \frac{j^n \varepsilon_n}{H^{(2)}_n(k_o a)} \cos\, n(\phi_p - \phi_i)\,. \qquad (2.36)$$

The matrix equation (2.34) can be solved to obtain numerical values for b_q, while (2.26) and (2.27) are employed to determine the unknown coefficients A_n and B_n, respectively.

CHAPTER 3

ANALYSIS OF SCATTERING BY A PERFECTLY CONDUCTING MULTI-SLOTTED CIRCULAR CYLINDER

In this chapter, the problem of scattering by a perfectly conducting circular cylinder with multi-slots is presented. The analysis developed in Chapter 2 for a single-slot cylinder is extended to solve for the problem of a multi-slot conducting cylinder.

The cylinder is assumed to have N-slots, each of an arbitrary slot width. Similar to the analysis used in Chapter 2, two methods are used to analize the problem under consideration. Starting with Maxwell's equations and the technique of separation of variables, the transmitted and scattered field unknown coefficients are found in terms of the assumed tangential aperture electric field. Continuity of the tangential magnetic field components across the N-apertures using the boundary value technique leads to the use of Galerkin's method. N-coupled equations containing the information of the N-slots are generated and solved simultaneously for the unknown aperture fields. In the second method, the continuity of the tangential magnetic field components across the apertures yields N-integral equations in terms

of the unknown aperture fields. The method of moments is introduced in order to solve these integral equations, where the unknown aperture fields are expressed in terms of an infinite series with a linear combination of the expansion functions. The expansion functions are then substituted into the integral equations, then weighting functions are defined and used to test each integral equation at different points.

3.1 Boundary Value Method

Consider a perfectly conducting circular cylinder of radius a, with N-axial slots along the z-axis, each of angular width $\Delta\phi_j = \beta_j - \alpha_j$, where the subscript j denotes the aperture index. The inner region of the cylinder is assumed filled with a dielectric material of permittivity ε_1 and permeability μ_1, and the outer region is taken to be free space. The cylinder is excited by a z-polarized transverse magnetic TM_z plane wave, with incidence angel ϕ_i measured from the positive x-axis, as shown in Fig. 3.1. Since the source and structure are independent of z, the fields produced by this source can only have z-component of the electric field that do not vary with z. Using Maxwell's equations and following the formulation in Chapter 2, the total electric field components in both regions are given by

$$E_z^1 = \sum_{n=0}^{\infty} j^n \varepsilon_n A_n J_n(k_1\rho)\cos n\phi \qquad \rho < a \quad (3.1)$$

$$E_z^2 = \sum_{n=0}^{\infty} j^n \varepsilon_n \left[B_n H_n^{(2)}(k_o\rho) + J_n(k_o\rho)\right]\cos n(\phi - \phi_i) \qquad \rho > a \quad (3.2)$$

The total ϕ components of the corresponding magnetic field can readily be found from (2.2).

$$H_\phi^1 = -jy_1 \sum_{n=0}^{\infty} j^n \varepsilon_n A_n J_n'(k_1\rho)\cos n\phi \qquad \rho < a \quad (3.3)$$

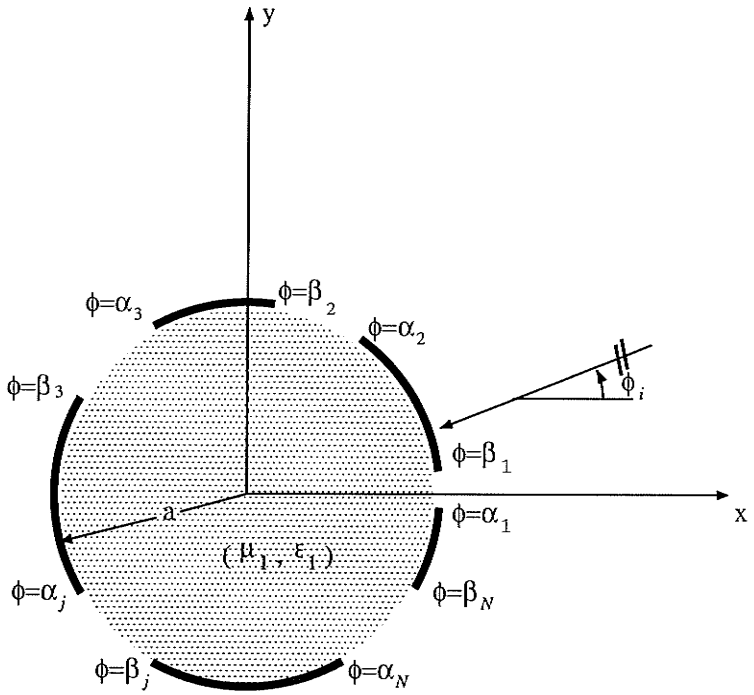

Figure 3.1: Geometry of the multi-slot problem.

$$H_\phi^2 = -jy_o \sum_{n=0}^{\infty} j^n \varepsilon_n \left[B_n H_n'^{(2)}(k_o\rho) + J_n'(k_o\rho) \right] \cos n(\phi - \phi_i) \quad \rho > a \quad (3.4)$$

Here, J_n is the cylindrical Bessel function of order n, $H_n^{(2)}$ is the cylindrical Hankel function of the second kind and order n. The prime superscript denotes differentiation with respect to the total argument, y_o and y_1 are the intrinsic admittance of free space and dielectric material, respectively, while A_n are the transmitted field coefficients and B_n are the scattered field coefficients.

To solve for the unknown transmitting and scattering field coefficients A_n and B_n, respectively, the following boundary conditions have to be satisfied.

$$E_z^1 = \begin{cases} E_j(\phi) & \alpha_j < \phi < \beta_j \qquad j = 1, 2, ..., N \\ 0 & \text{otherwise} \end{cases} \qquad \text{at} \quad \rho = a \qquad (3.5)$$

$$E_z^2 = \begin{cases} E_j(\phi) & \alpha_j < \phi < \beta_j \qquad j = 1, 2, ..., N \\ 0 & \text{otherwise} \end{cases} \qquad \text{at} \quad \rho = a \qquad (3.6)$$

and

$$H_\phi^1 = H_\phi^2 \qquad 0 \leq \phi \leq 2\pi \qquad \text{at} \quad \rho = a \qquad (3.7)$$

Continuity of the tangential electric fields can be accomplished by expanding the unknown aperture fields $E_j(\phi)$ in terms of a complete set of orthogonal functions defined on their respective domains. The expansion function has to be of ϕ dependence only and z-directed. Also, it needs to be chosen so as to conform with the edge conditions at $\rho = a$, $\phi = \alpha_j$ and $\phi = \beta_j$. Moreover, the choice has to be

appropriate in a way to make the integrals involved in the formulation possible to evaluate.

Continuity of the tangential electric fields at $\rho = a$ leads to

$$\sum_{n=0}^{\infty} j^n \varepsilon_n A_n J_n(k_1 a) \cos\, n\phi = \begin{cases} E_j(\phi) & \alpha_j < \phi < \beta_j \\ 0 & \text{otherwise} \end{cases} \tag{3.8}$$

and

$$\sum_{n=0}^{\infty} j^n \varepsilon_n \left[B_n H_n^{(2)}(k_o a) + J_n(k_o a) \right] \cos\, n(\phi - \phi_i) = \begin{cases} E_j(\phi) & \alpha_j < \phi < \beta_j \\ 0 & \text{otherwise} \end{cases} . \tag{3.9}$$

Next, we choose

$$E_j(\phi) = \sum_{q_j=1}^{\infty} a_{q_j} \sin \gamma_j(\phi - \alpha_j) \tag{3.10}$$

where $E_j(\phi)$ is the j^{th} unknown aperture field, a_{q_j} are the unknown complex expansion coefficients of the j^{th} aperture, and $\gamma_j = \pi q_j/(\beta_j - \alpha_j)$

Substituting (3.10) into (3.8) and (3.9) and making use of the orthogonality property of the trigonometric function, one obtains the transmitted field coefficients as follows.

$$A_n = \frac{j^{-n}}{\pi \varepsilon_n} \frac{1}{J_n(k_1 a)} \sum_{j=1}^{N} \sum_{q_j=1}^{\infty} a_{q_j} F_{q_j n} \tag{3.11}$$

where

$$F_{q_j n} = \int_{\alpha_j}^{\beta_j} \sin \gamma_j(\phi - \alpha_j) \cos\, n\phi \, d\phi \,. \tag{3.12}$$

The scattered field coefficients become

$$B_n = \frac{1}{H_n^{(2)}(k_o a)} \left[\frac{j^{-n}}{\pi \varepsilon_n} \sum_{j=1}^{N} \sum_{q_j=1}^{\infty} a_{q_j} G_{q_j n} - J_n(k_o a) \right] \tag{3.13}$$

where

$$G_{q_j n} = \int_{\alpha_j}^{\beta_j} \sin \gamma_j(\phi - \alpha_j) \cos\, n(\phi - \phi_i)\, d\phi\,. \tag{3.14}$$

Similarly, application of the continuity of the tangential magnetic field components (3.7) leads to the following equation.

$$y_1 \sum_{n=0}^{\infty} j^n \varepsilon_n A_n J_n'(k_1 a) \cos\, n\phi = y_o \sum_{n=0}^{\infty} j^n \varepsilon_n \left[B_n H_n'^{(2)}(k_o a) + J_n'(k_o a)\right] \cdot \cos\, n(\phi - \phi_i) \tag{3.15}$$

Substituting (3.11) and (3.13) into (3.15) and making use of the Wronskian determinant

$$J_n'(x) H_n^{(2)}(x) - H_n'^{(2)}(x) J_n(x) = \frac{2j}{\pi x} \tag{3.16}$$

one obtains

$$\sum_{j=1}^{N} \sum_{q_j=1}^{\infty} a_{q_j} \sum_{n=0}^{\infty} \left[\frac{y_1}{y_o} \frac{J_n'(k_1 a)}{J_n(k_1 a)} F_{q_j n} \cos\, n\phi - \frac{H_n'^{(2)}(k_o a)}{H_n^{(2)}(k_o a)} G_{q_j n} \cos\, n(\phi - \phi_i)\right] = \frac{2j}{k_o a} \sum_{n=0}^{\infty} \frac{j^n \varepsilon_n}{H_n^{(2)}(k_o a)} \cos\, n(\phi - \phi_i)\,. \tag{3.17}$$

In order for (3.17) to be evaluated for the unknown expansion coefficients a_{q_j}, Galerkin's technique has to be employed. Multiplying both sides of (3.17) by the corresponding weighting function of each aperture and integrating over each aperture independently, gives

$$\sum_{j=1}^{N} \sum_{q_j=1}^{\infty} a_{q_j} \sum_{n=0}^{\infty} \left[\frac{y_1}{y_o} \frac{J_n'(k_1 a)}{J_n(k_1 a)} F_{q_j n} F_{p_1 n} - \frac{H_n'^{(2)}(k_o a)}{H_n^{(2)}(k_o a)} G_{q_j n} G_{p_1 n}\right] = \frac{2j}{k_o a} \sum_{n=0}^{\infty} \frac{j^n \varepsilon_n}{H_n^{(2)}(k_o a)} G_{p_1 n}$$

$$\sum_{j=1}^{N}\sum_{q_j=1}^{\infty} a_{q_j} \sum_{n=0}^{\infty}\left[\frac{y_1}{y_o}\frac{J_n'(k_1a)}{J_n(k_1a)}F_{q_jn}F_{p_2n} - \frac{H_n'^{(2)}(k_oa)}{H_n^{(2)}(k_oa)}G_{q_jn}G_{p_2n}\right] = \frac{2j}{k_oa}\sum_{n=0}^{\infty}\frac{j^n\varepsilon_n}{H_n^{(2)}(k_oa)}G_{p_2n}$$

$$\vdots \qquad \vdots \qquad \vdots \qquad (3.18)$$

$$\sum_{j=1}^{N}\sum_{q_j=1}^{\infty} a_{q_j} \sum_{n=0}^{\infty}\left[\frac{y_1}{y_o}\frac{J_n'(k_1a)}{J_n(k_1a)}F_{q_jn}F_{p_Nn} - \frac{H_n'^{(2)}(k_oa)}{H_n^{(2)}(k_oa)}G_{q_jn}G_{p_Nn}\right] = \frac{2j}{k_oa}\sum_{n=0}^{\infty}\frac{j^n\varepsilon_n}{H_n^{(2)}(k_oa)}G_{p_Nn}$$

In matching H_ϕ across the aperture, a selection of the weighting functions was made to be the same as the basis function in (3.10). Where $\sin\gamma_{j'}(\phi-\alpha)$ is the weighting function of the j^{th} aperture, and $\gamma_{j'} = \pi p_{j'}/(\beta_{j'}-\alpha_{j'})$ and j' represents the index of the j^{th} weighting function which corresponds to the j^{th} aperture. Now, (3.19) can be written in a matrix form as follows

$$\sum_{j'=1}^{N}\left[Z_{p_{j'}q_j}\right]\left[a_{q_j}\right] = \sum_{j'=1}^{N}\left[V_{p_{j'}}\right] \qquad (3.19)$$

a_{q_j} in (3.19) represent the unknown fields expansion coefficients of the j^{th} aperture where

$$Z_{p_{j'}q_j} = \sum_{n=0}^{\infty}\left[\frac{y_1}{y_o}\frac{J_n'(k_1a)}{J_n(k_1a)}F_{q_jn}F_{p_{j'}n} - \frac{H_n'^{(2)}(k_oa)}{H_n^{(2)}(k_oa)}G_{q_jn}G_{p_{j'}n}\right] \qquad (3.20)$$

$$V_{p_{j'}} = \frac{2j}{k_oa}\sum_{n=0}^{\infty}\frac{j^n\varepsilon_n}{H_n^{(2)}(k_oa)}G_{p_{j'}n}\,. \qquad (3.21)$$

The matrix equation in (3.19) can be solved to obtain numerical values for a_{q_j}, while (3.11) and (3.13) are employed to determine the unknown coefficients A_n and B_n respectively.

3.2 Aperture Field Integral Equation

Following the same analysis discussed in Section 3.1, the electric and magnetic field components in both regions will have the same expansion forms as given by (2.6–2.9). By enforcing the continuity of the tangential electric field (3.5–3.6), and making use of the orthogonality property of the trigonometric functions, we obtain the transmitting and scattering field coefficients in an integral form as follows

$$A_n = \frac{j^{-n}}{\pi\varepsilon_n}\frac{1}{J_n(k_1a)}\sum_{j=1}^{N}\int_{\alpha_j}^{\beta_j} E_j(\phi')\cos n\phi'\,d\phi' \tag{3.22}$$

$$B_n = \frac{1}{H_n^{(2)}(k_oa)}\left[\frac{j^{-n}}{\pi\varepsilon_n}\sum_{j=1}^{N}\int_{\alpha_j}^{\beta_j} E_j(\phi')\cos n(\phi'-\phi_i)\,d\phi' - J_n(k_oa)\right] \tag{3.23}$$

Now, applying the remaining boundary condition (3.7) and substituting for A_n and B_n into (3.15) one gets an integral equation as follows

$$\sum_{n=0}^{\infty}\sum_{j=1}^{N}\int_{\alpha_j}^{\beta_j}\left[\frac{y_1}{y_o}\frac{J_n'(k_1a)}{J_n(k_1a)}\cos n\phi\cos n\phi' - \frac{H_n'^{(2)}(k_oa)}{H_n^{(2)}(k_oa)}\cos n(\phi-\phi_i)\cos n(\phi'-\phi_i)\right] \cdot E_j(\phi')\,d\phi' = \frac{2j}{k_oa}\sum_{n=0}^{\infty}\frac{j^n\varepsilon_n}{H_n^{(2)}(k_oa)}\cos n(\phi-\phi_i). \tag{3.24}$$

where ϕ' is a dummy variable of integration.

Equation (3.24) represents the aperture integral equation. This equation as discussed in Section 2.2.1, is of no use unless it can be evaluated for the unknown quantity. One way to solve this integral equation is numerically. Method of moments [21] has proven to be the most efficient approximate method for obtaining result of acceptable accuracy. The technique of method of moments is discussed in Section 2.2.1.

Now, in order to use the method of moments to solve the integral equation (3.24), the aperture fields $E_j(\phi)$ will be expanded as a series of basis functions and unknown complex expansion coefficients such as

$$E_j(\phi) = \sum_{q_j=1}^{Q} b_{q_j} M_{q_j} \tag{3.25}$$

where b_{q_j} are the unknown complex coefficients of the j^{th} aperture, and M_{q_j} are known basis functions of the corresponding aperture. Substituting (3.25) back into (3.24) and choosing the j^{th} basis functions as pulse functions such as

$$M_{q_j} = \delta(\phi - \phi_{q_j}) = \begin{cases} 1 & \phi = \phi_{q_j} \\ 0 & \text{otherwise} \end{cases} \qquad \phi_{q_j} \in \Delta\phi_j \,. \tag{3.26}$$

A simple way to obtain an approximate solution is to require that equation (3.24) be satisfied at discrete points in the corresponding aperture. This procedure is a part of the point-matching method. To achieve this, a set of testing functions $W_{p_{j'}}$ correspond to the j^{th} aperture are selected as follows

$$W_{p_{j'}} = \delta(\phi - \phi_{p_{j'}}) = \begin{cases} 1 & \phi = \phi_{p_{j'}} \\ 0 & \text{otherwise} \end{cases} \,. \tag{3.27}$$

Next, define an inner product as in [21]

$$< W, G > = \int_{s_j} W \cdot G \, ds \tag{3.28}$$

where s_j is the j^{th} aperture width. Finally, Equation (3.24) can be written in a matrix form as follows.

$$\sum_{j'=1}^{N} \left[Z'_{p_{j'} q_j} \right] \left[b_{q_j} \right] = \sum_{j'=1}^{N} \left[V'_{p_{j'}} \right] , \tag{3.29}$$

where

$$Z'_{p_{j'}q_j} = \sum_{n=0}^{\infty} \left[\frac{y_1}{y_o} \frac{J'_n(k_1 a)}{J_n(k_1 a)} \cos\, n\phi_{q_j} \cos\, n\phi_{p_{j'}} - \frac{H'^{(2)}_n(k_o a)}{H^{(2)}_n(k_o a)} \cos\, n(\phi_{q_j} - \phi_i) \right.$$
$$\left. \cdot \cos\, n(\phi_{p_{j'}} - \phi_i) \right] \quad (3.30)$$

and

$$V'_{p_{j'}} = \frac{2j}{k_o a} \sum_{n=0}^{\infty} \frac{j^n \varepsilon_n}{H^{(2)}_n(k_o a)} \cos\, n(\phi_{p_{j'}} - \phi_i)\,. \quad (3.31)$$

The matrix equation (3.29) can be solved to obtain numerical values for b_{q_j} while (3.22) and (3.23) are employed to determine the unknown coefficients A_n and B_n, respectively.

CHAPTER 4

RESULTS AND DISCUSSION FOR THE SINGLE-SLOT CASE

This chapter presents numerical results for the single-slot case. The results are classified into three sections. The first is used to examine the accuracy of the solution over the boundary region, and to check the validity of the solution for the complete conducting case. The second section discusses the results for the far scattered field of a single slot case with an arbitrary slot angle. Finally, the results for the bistatic scattering width are discussed in the last section. Using (2.23) and (2.34) to solve for a_q and b_q respectively, the transmitted and scattered field coefficients can be obtained as given in Chapter 2. The bistatic scattering width can be found as

$$\sigma(\phi) = \lim_{\rho \to \infty} 2\pi\rho \left| \frac{E^s(\rho, \phi)}{E_i} \right|^2 \tag{4.1}$$

4.1 Comparison Results

To examine the accuracy of the solution over the boundary region, the tangential component of the total electric field (E_z^1) and (E_z^2) were computed using (2.6) and (2.7),respectively with $\phi_i = 0^o$, while the cylinder is taken to have an electric radius $ka = 2\pi$, and relative permittivity $\varepsilon_r = 1$. The results for two different

slot angles are shown in Fig. 4.1, where $\alpha = -5^o$ and $\beta = 5^o$, and Fig. 4.2 where $\alpha = -25^o$ and $\beta = 25^o$. Both figures show a very good agreement between the two proposed methods and confirm that the total tangential electric field vanishes at the conducting surface. Moreover, both (2.6) and (2.7) gave the same results for the surface tangential electric field. Fig. 4.3 shows the bistatic scattering width for a complete conducting cylinder in comparison with a slotted cylinder of an infinite relative permittivity and the realtive permeability approaching 0. The cylinder has an electric radius $ka = 2\pi$ and a slot angle of 50^o. Similarly, Fig. 4.4 compares the results of the bistatic scattering width of a complete conducting cylinder with a very narrow-slot cylinder. It can be concluded that the proposed methods are in a very good agreement with the exact solution of the complete conducting cylinder.

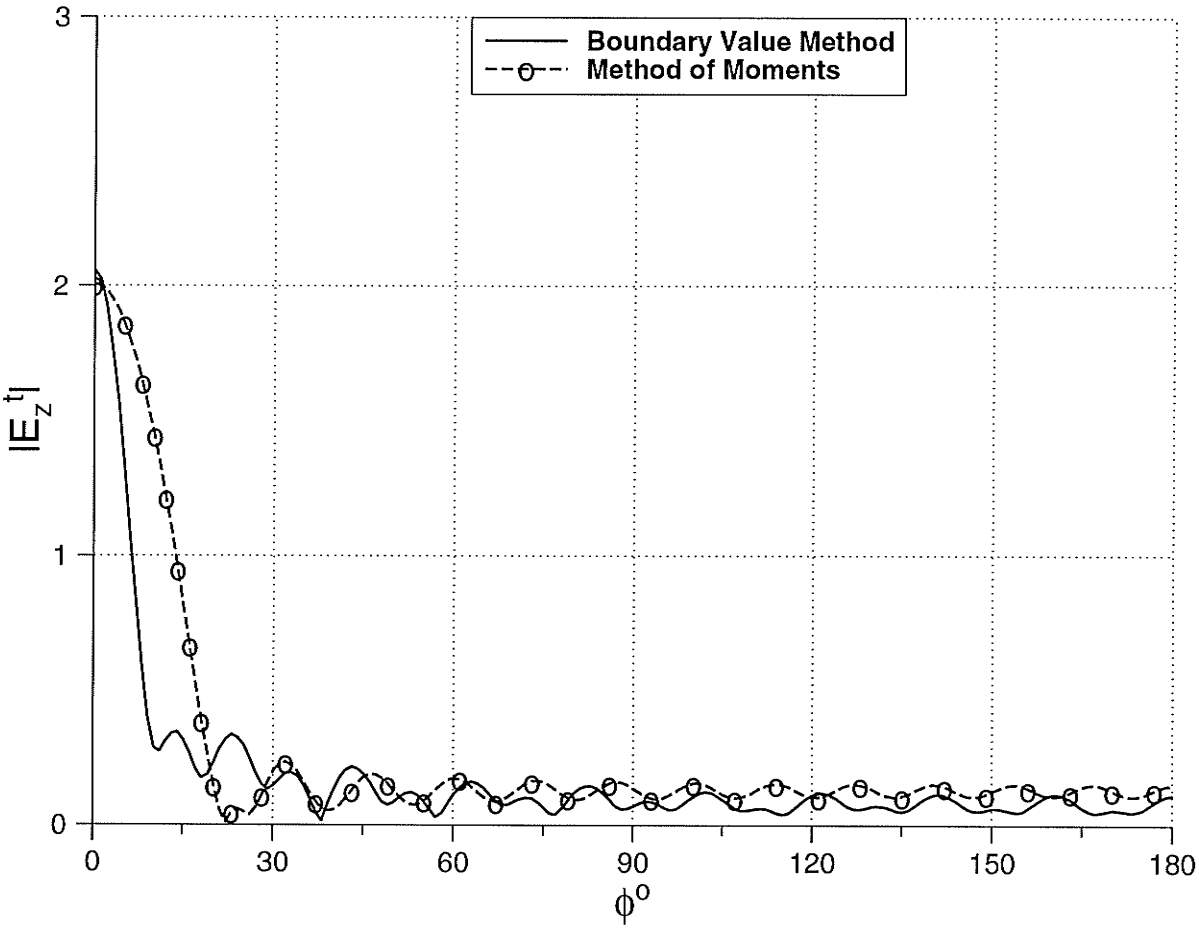

Figure 4.1: Total tangential electric field with $ka = 2\pi$, $\varepsilon_r = 1$, $\phi_i = 0^o$, $\alpha = -5^o$ and $\beta = 5^o$.

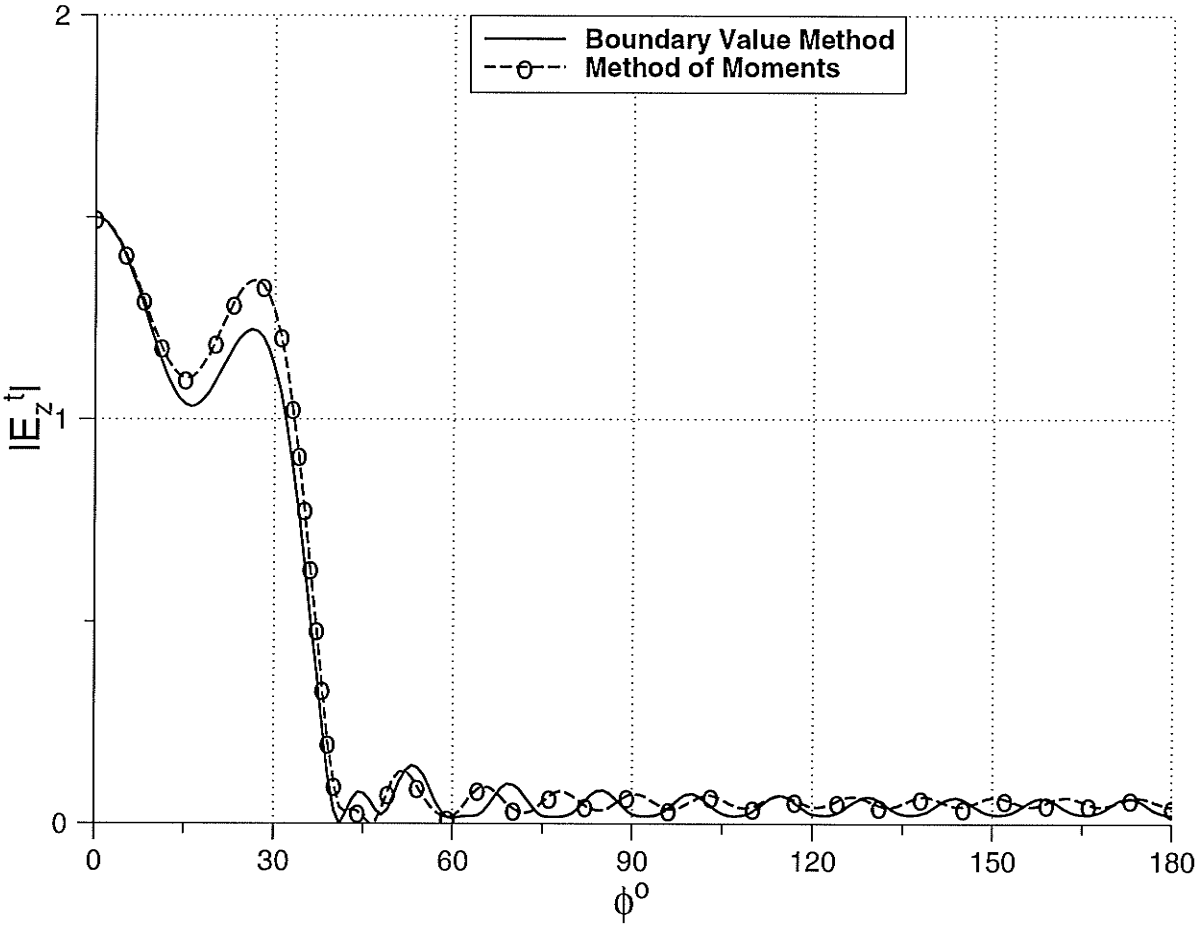

Figure 4.2: Total tangential electric field with $ka = 2\pi$, $\varepsilon_r = 1$, $\phi_i = 0^o$, $\alpha = -25^o$ and $\beta = 25^o$.

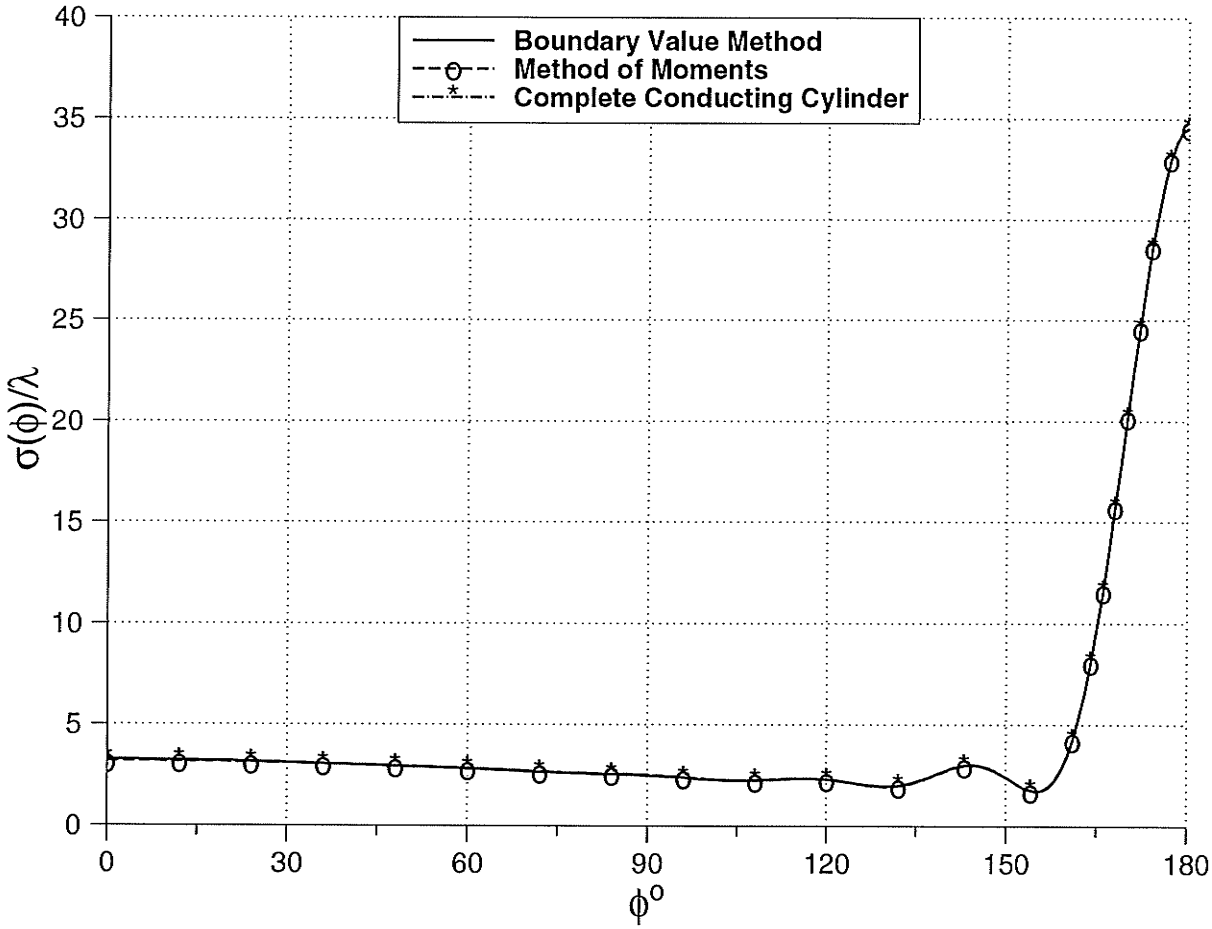

Figure 4.3: Comparison of bistatic scattering width for a complete conducting cylinder with slotted cylinder, $\varepsilon_r = \infty$, $\phi_i = 0^o$, $\alpha = -5^o$ and $\beta = 5^o$.

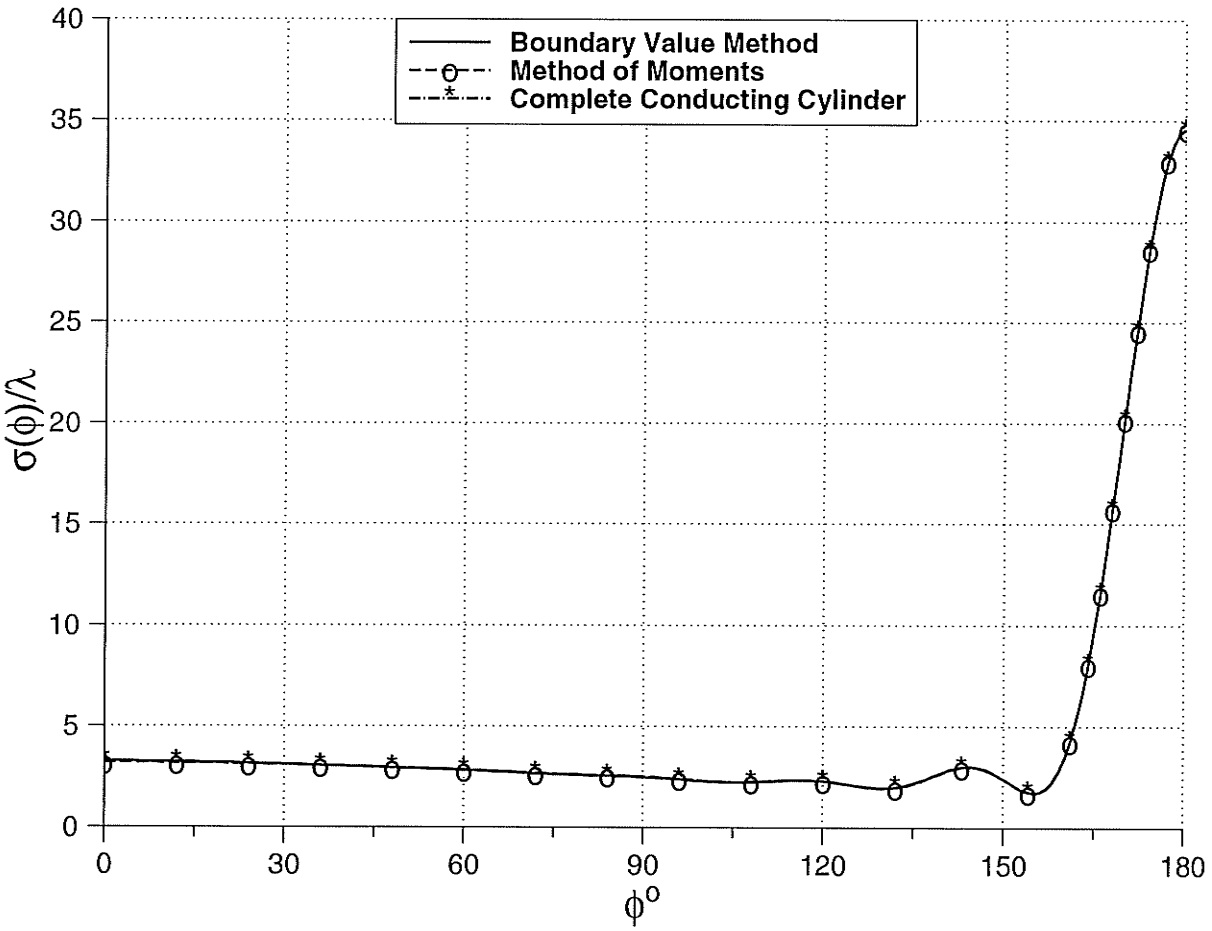

Figure 4.4: Comparison of bistatic scattering width for a complete conducting cylinder with a narrow slot cylinder, $\varepsilon_r = 1$, $\phi_i = 0^o$, $\alpha = -1/2^o$ and $\beta = 1/2^o$.

4.2 Results for the Far Scattered Field

This section discusses the behavior of the far scattered field for the single slot case. The results are plotted for an arbitrary slots angle and incidence angle. The far scattered field can be obtained using (2.7).

Figs. 4.5–4.8 show the result of the far scattered field for a slot angle of 10^o i.e. $(\alpha = -5^o, \beta = 5^o)$ and an arbitrary incidence angle $\phi_i = 0^o, 90^o, 180^o, 270^o$, respectively. Fig. 4.9 and Fig. 4.10 show the far scattered field for the same problem where $\alpha = 175^o$ and $\beta = 185^o$ and for incidence angles of $\phi_i = 0^o, 180^o$ respectively. It can be concluded that the maximum far scattered field occurs in the forward direction, and the direction of the incident field affects the strength of the maximum scattered field and number of the oscillations. Fig. 4.12 shows the results of the back scattering width using the two methods with slot angle of 10^o, from which it can be concluded that the maximum back scattering width takes place in the vicinity of the slot, (due to the edge effect), and it becomes almost constant as we move away from the aperture.

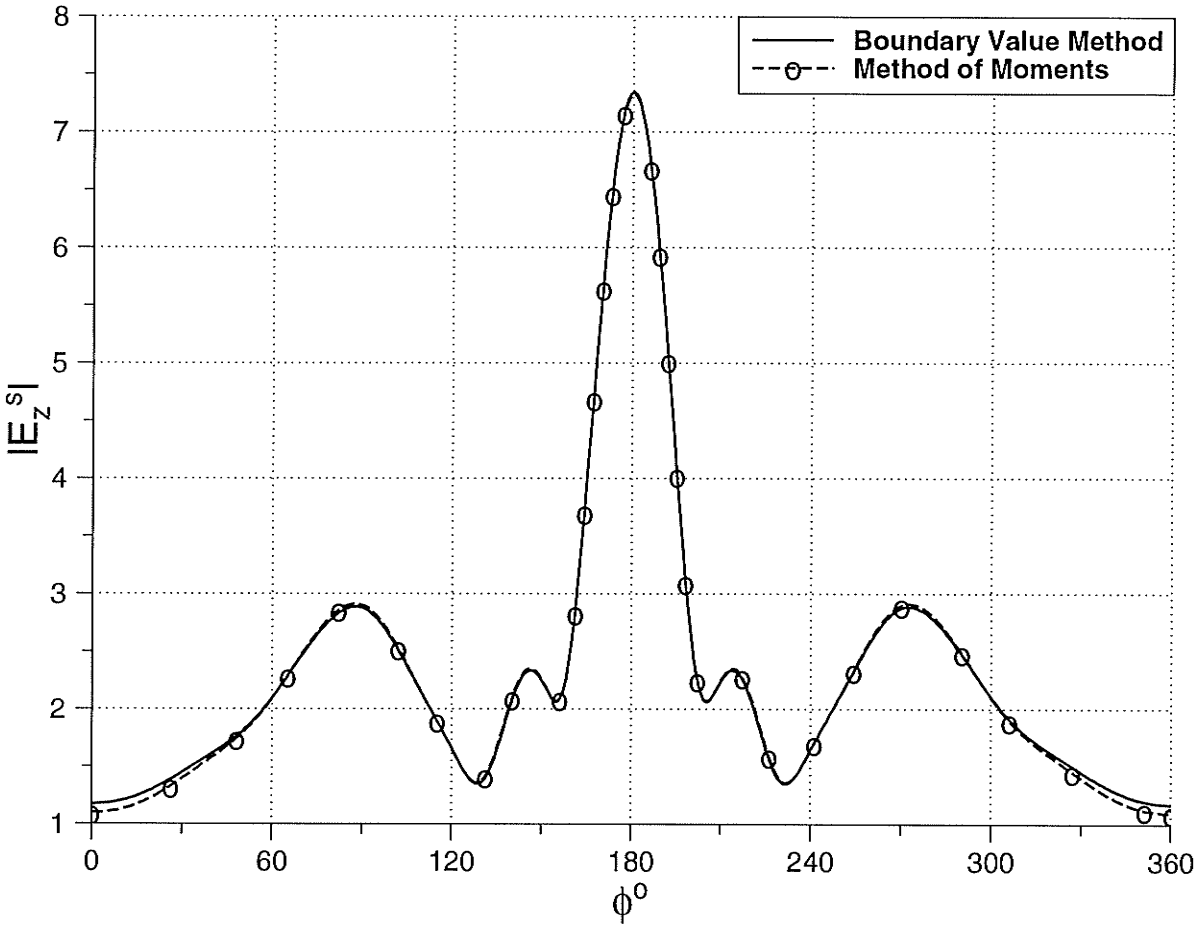

Figure 4.5: Far scattered field with $ka = 2\pi$, $\varepsilon_r = 1$, $\phi_i = 0^o$, $\alpha = -5^o$ and $\beta = 5^o$.

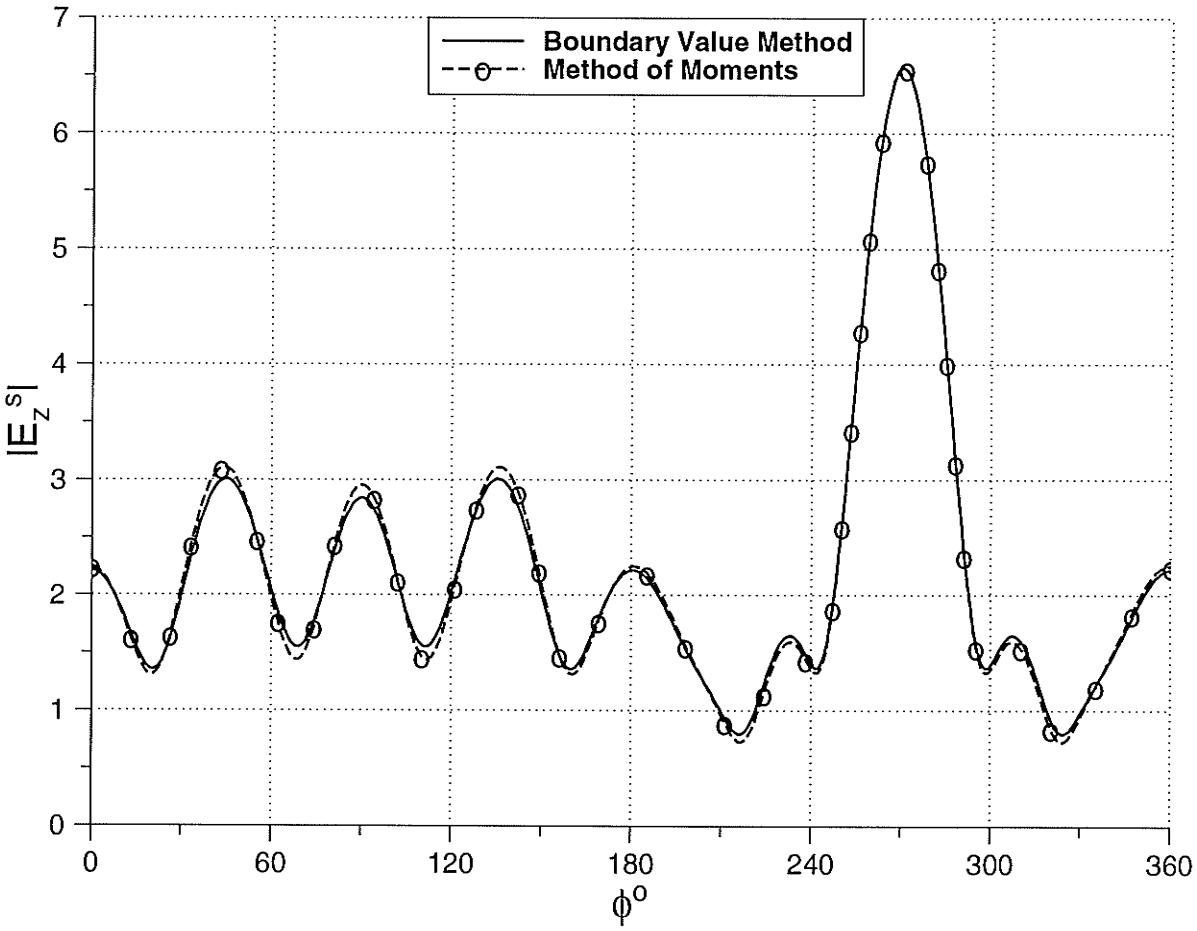

Figure 4.6: Far scattered field with $ka = 2\pi$, $\varepsilon_r = 1$, $\phi_i = 90^o$, $\alpha = -5^o$ and $\beta = 5^o$.

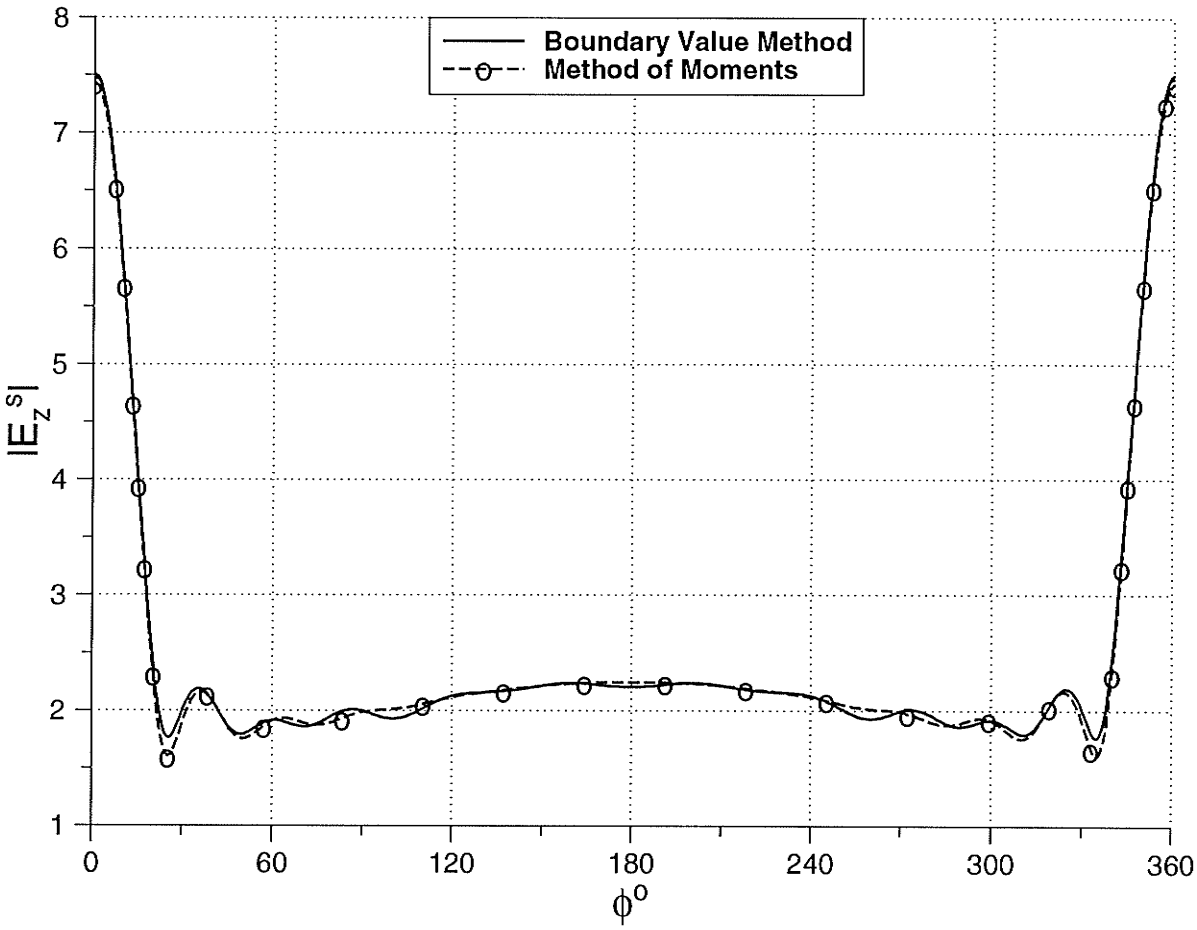

Figure 4.7: Far scattered field with $ka = 2\pi$, $\varepsilon_r = 1$, $\phi_i = 180^o$, $\alpha = -5^o$ and $\beta = 5^o$.

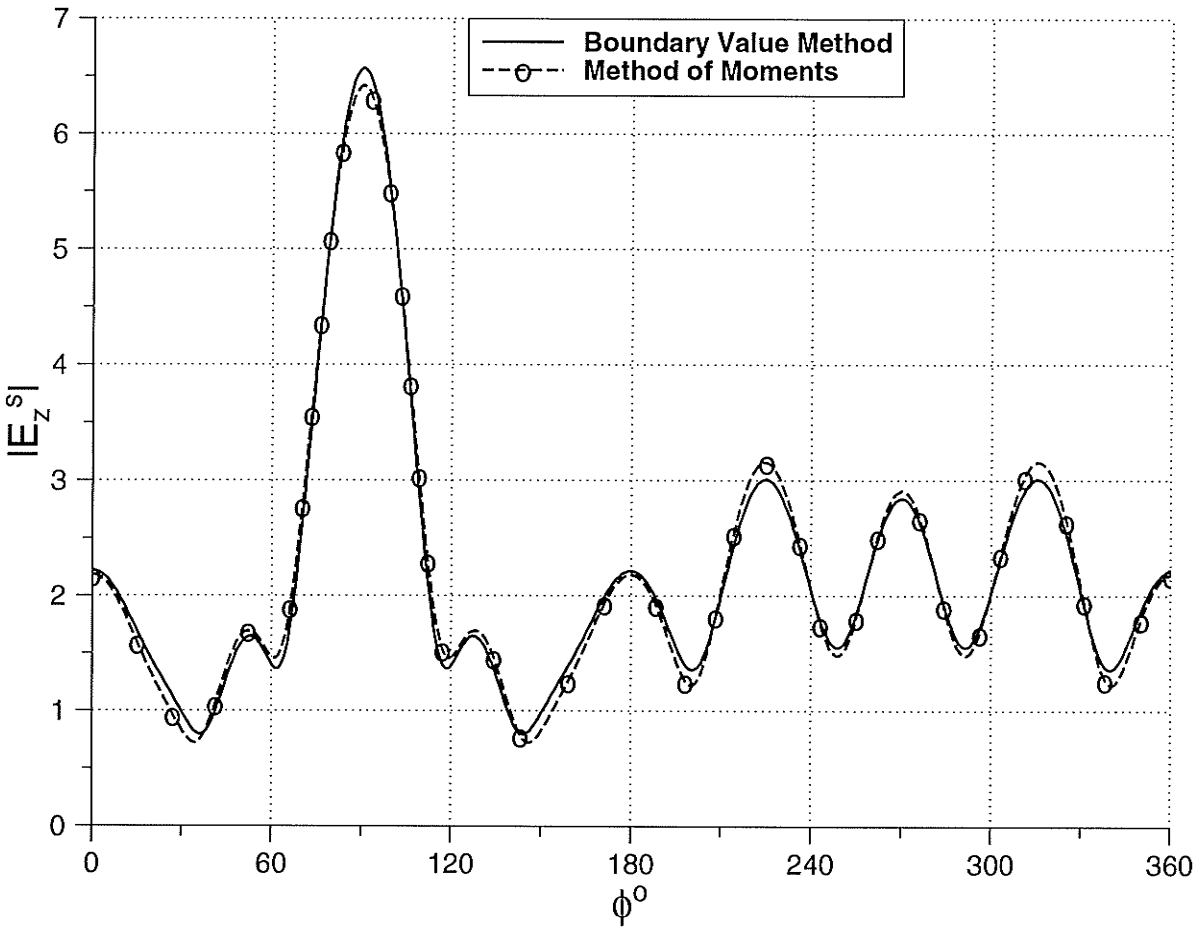

Figure 4.8: Far scattered field with $ka = 2\pi$, $\varepsilon_r = 1$, $\phi_i = 270^o$, $\alpha = -5^o$ and $\beta = 5^o$.

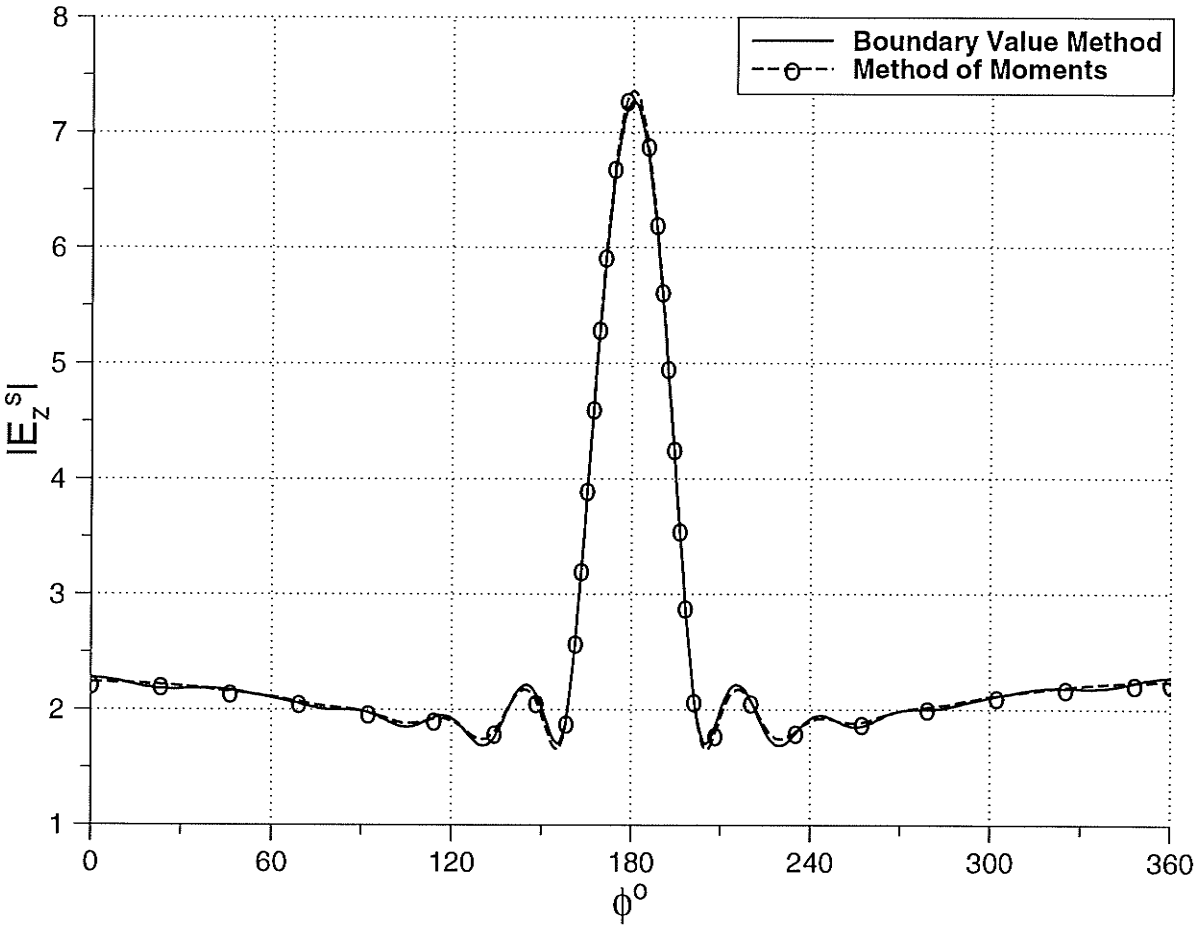

Figure 4.9: Far scattered field with $ka = 2\pi$, $\varepsilon_r = 1$, $\phi_i = 0^o$, $\alpha = 175^o$ and $\beta = 185^o$.

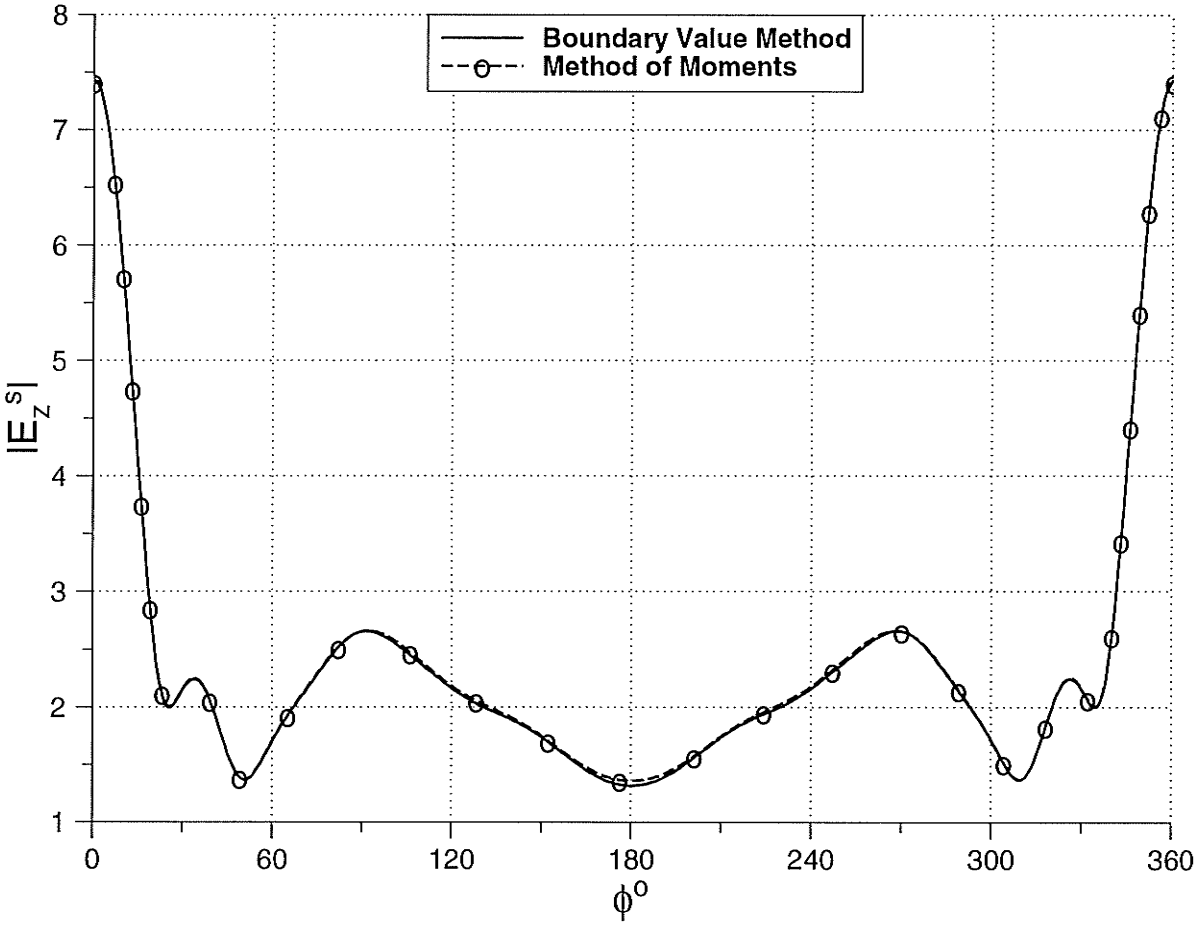

Figure 4.10: Far scattered field with $ka = 2\pi$, $\varepsilon_r = 1$, $\phi_i = 180^o$, $\alpha = 175^o$ and $\beta = 185^o$.

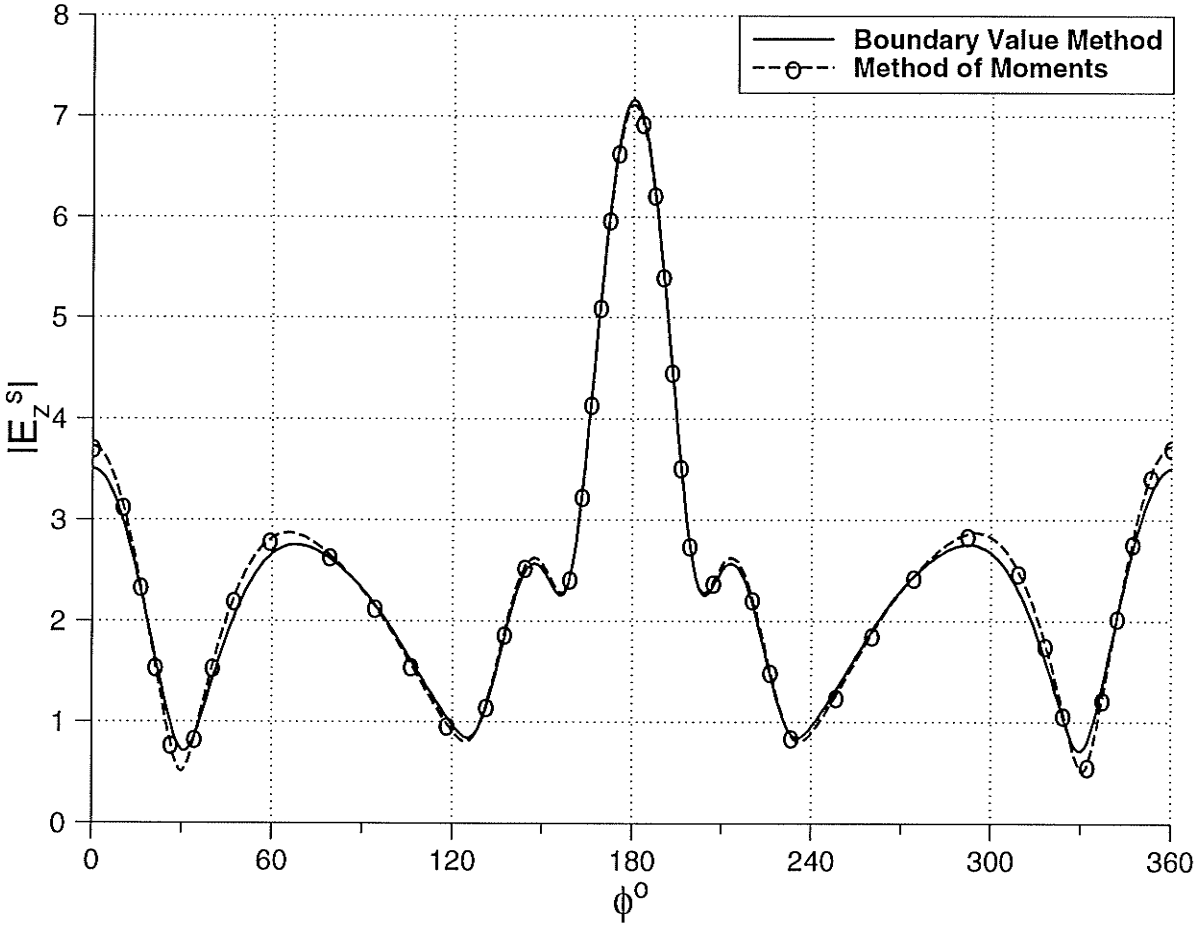

Figure 4.11: Far scattered field with $ka = 2\pi$, $\varepsilon_r = 1$, $\phi_i = 0^o$, $\alpha = -25^o$ and $\beta = 25^o$.

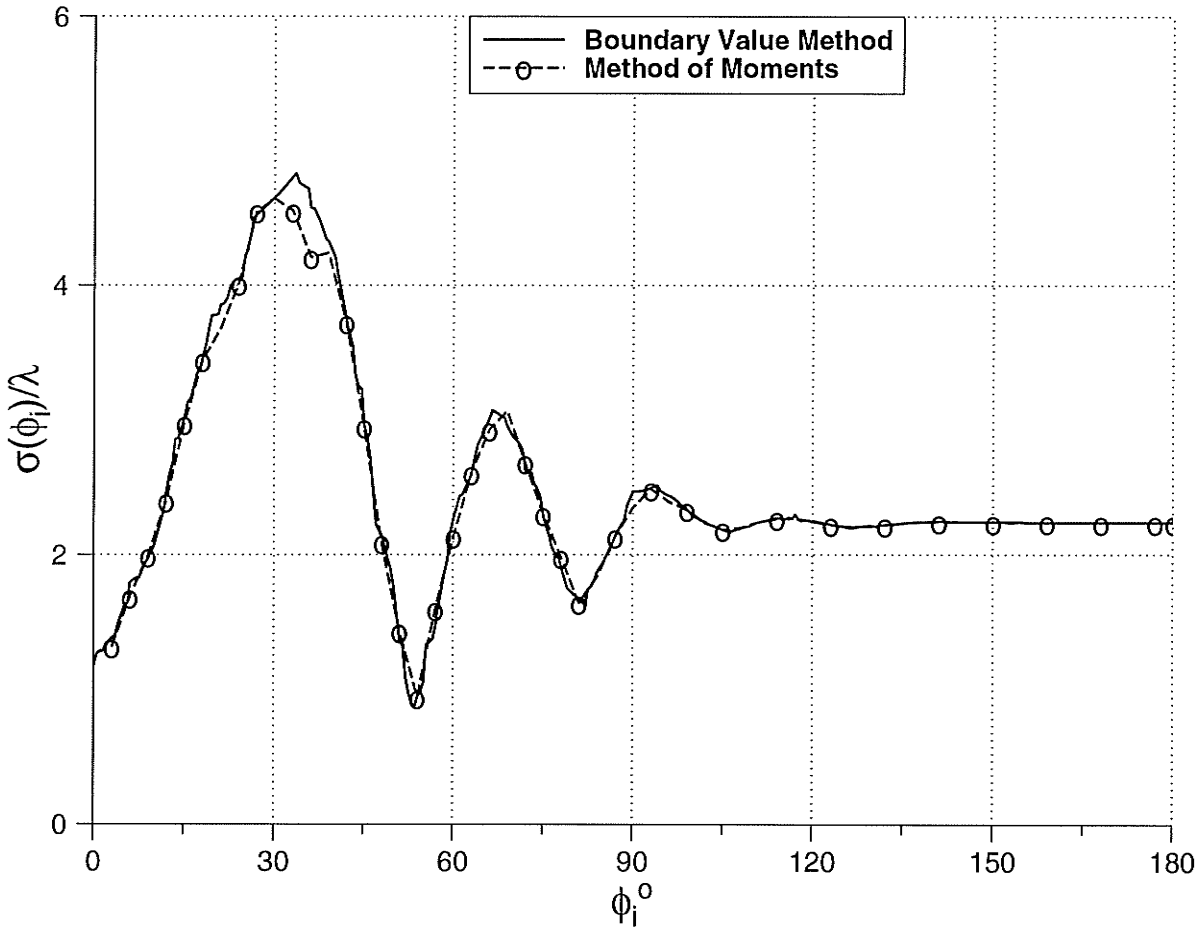

Figure 4.12: Back scattering width with $ka = 2\pi$, $\varepsilon_r = 1$, $\alpha = -5^o$ and $\beta = 5^o$.

4.3 Results for the Bistatic Scattering Width

The results for the bistatic scattering width for different slot angles and different slot positions are given in Figs. 4.13–4.14, from which it can be concluded that if the slot is in the opposite direction to the incident field, the bistatic scattering width would be smoother and would have less oscillations. Furthermore, as the size of the slot angle increases, the forward bistatic scattering width would decrease, the back bistatic scattering width would increase and the number of oscillations would increase also. The effect of loading the inner region of a slotted cylinder by a dielectric material of relative permittivity $\varepsilon_r = 3, 7, 11$ and a slot size of 50^o are shown in Figs. 4.15–4.17 respectively, it can be concluded that as the permittivity increases the response of the bistatic scattering width becomes smoother. Finally, Fig. 4.18 shows the results for the back scattering width with respect to the electrical radius ka of a cylinder with a 10^o slot i.e. ($\alpha = -5^o$ and $\beta = 5^o$), $\varepsilon_r = 1$ and $\phi_i = 0^o$, from which it is clear that as ka increases the back scattering width increases.Finally we can conclude that as the size of the slot or the radius of the cylinder increases more terms are required in order for the solution to converge. For example, for a cylinder of $ka = 2\pi$ and a slot angle of 10^o, 5 terms are needed in order for the boundary value solution to converge, while the aperture field integral equation solution requires 40 segments as a minimum in order for the solution to converge. Moreover, more sampling points are needed near the edges of the slot.

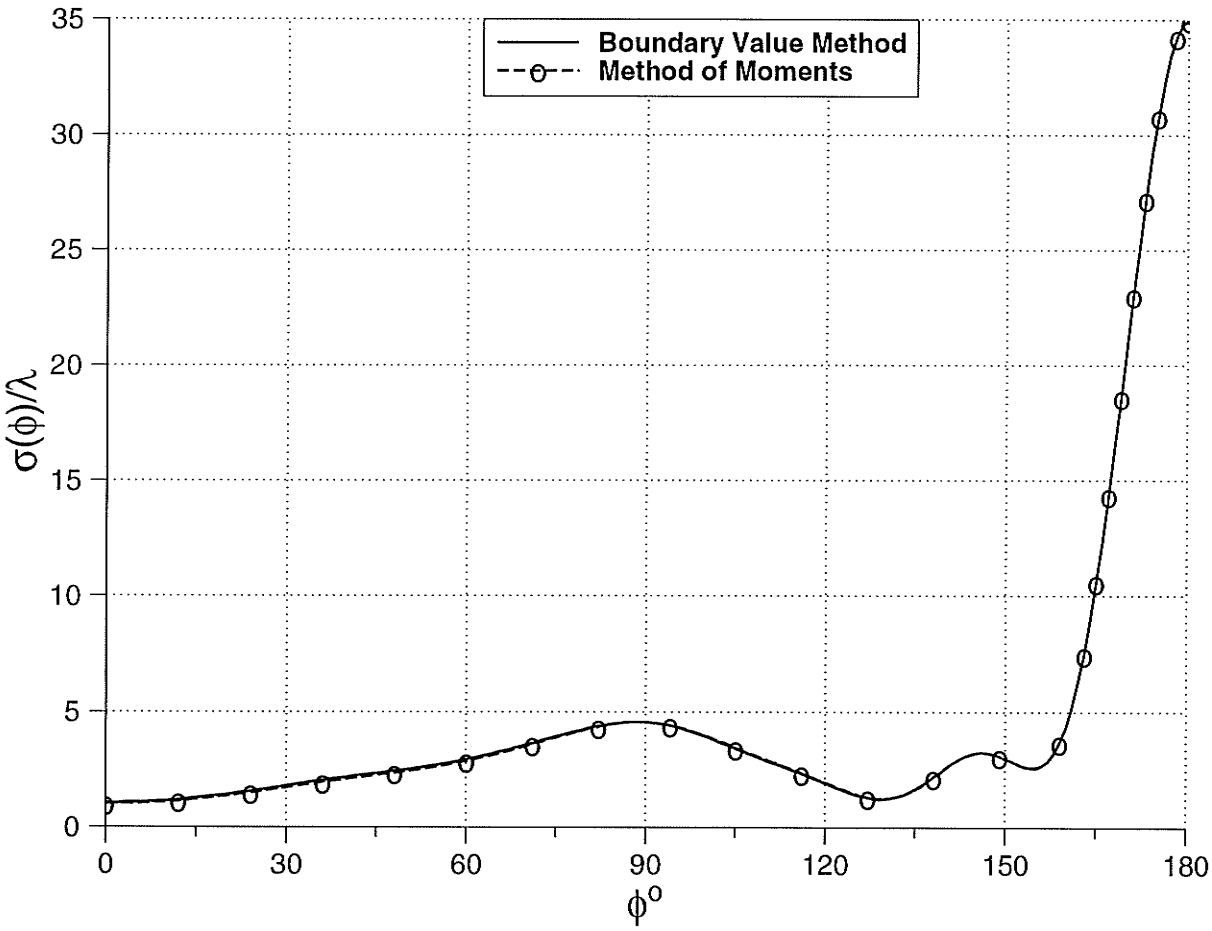

Figure 4.13: Bistatic scattering width with $ka = 2\pi$, $\varepsilon_r = 1$, $\phi_i = 0^o$, $\alpha = -5^o$ and $\beta = 5^o$.

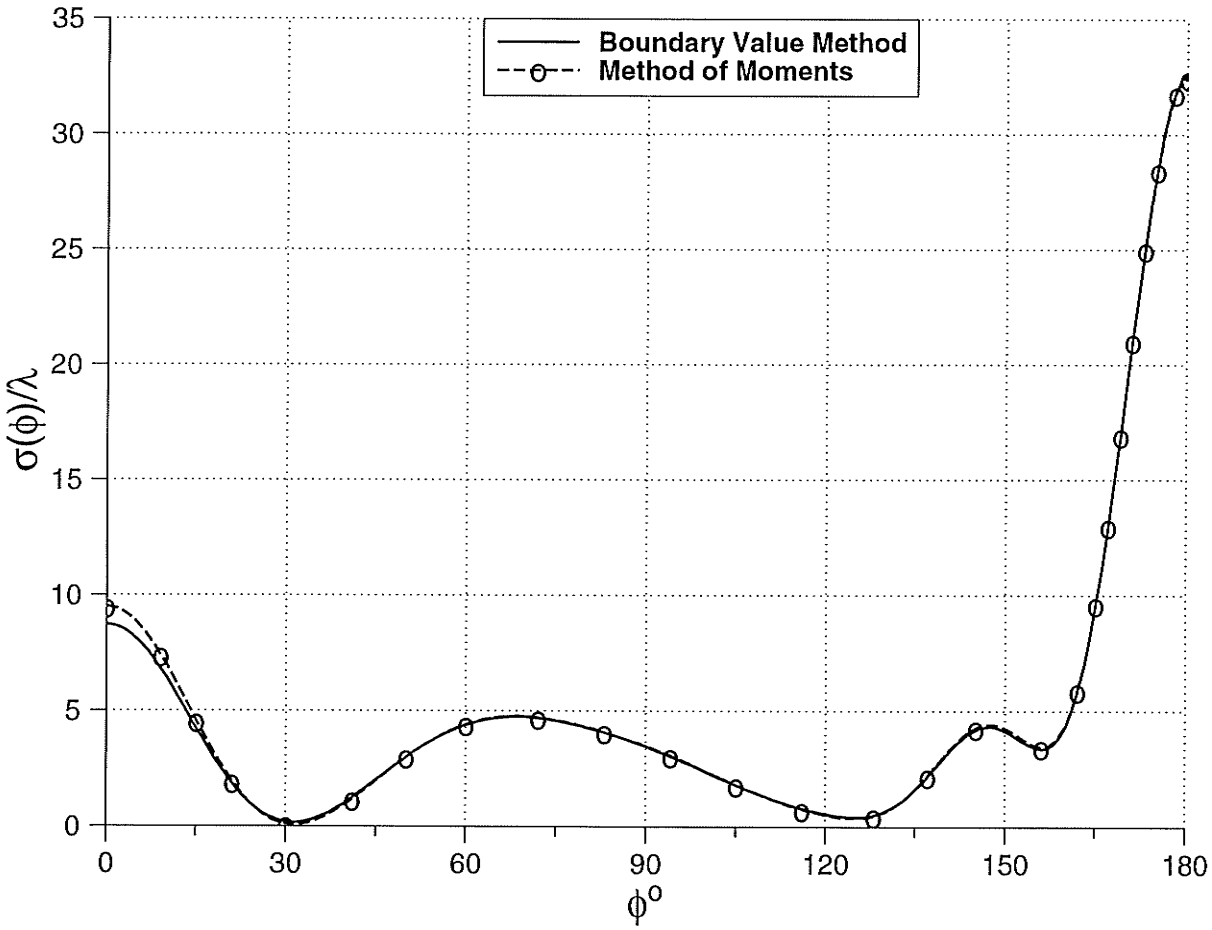

Figure 4.14: Bistatic scattering width with $ka = 2\pi$, $\varepsilon_r = 1$, $\phi_i = 0^o$, $\alpha = -25^o$ and $\beta = 25^o$.

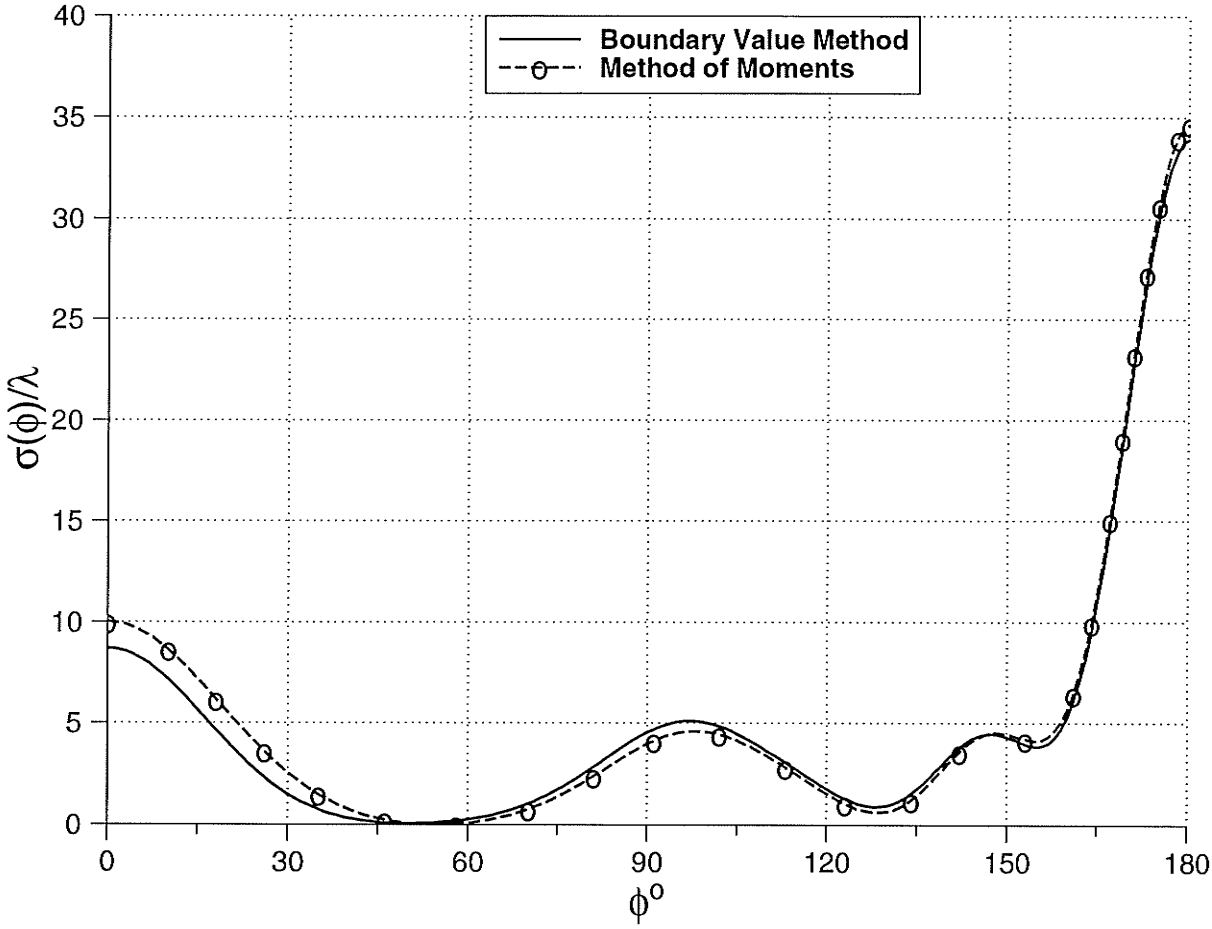

Figure 4.15: Bistatic scattering width with $ka = 2\pi$, $\varepsilon_r = 3$, $\phi_i = 0^o$, $\alpha = -25^o$ and $\beta = 25^o$.

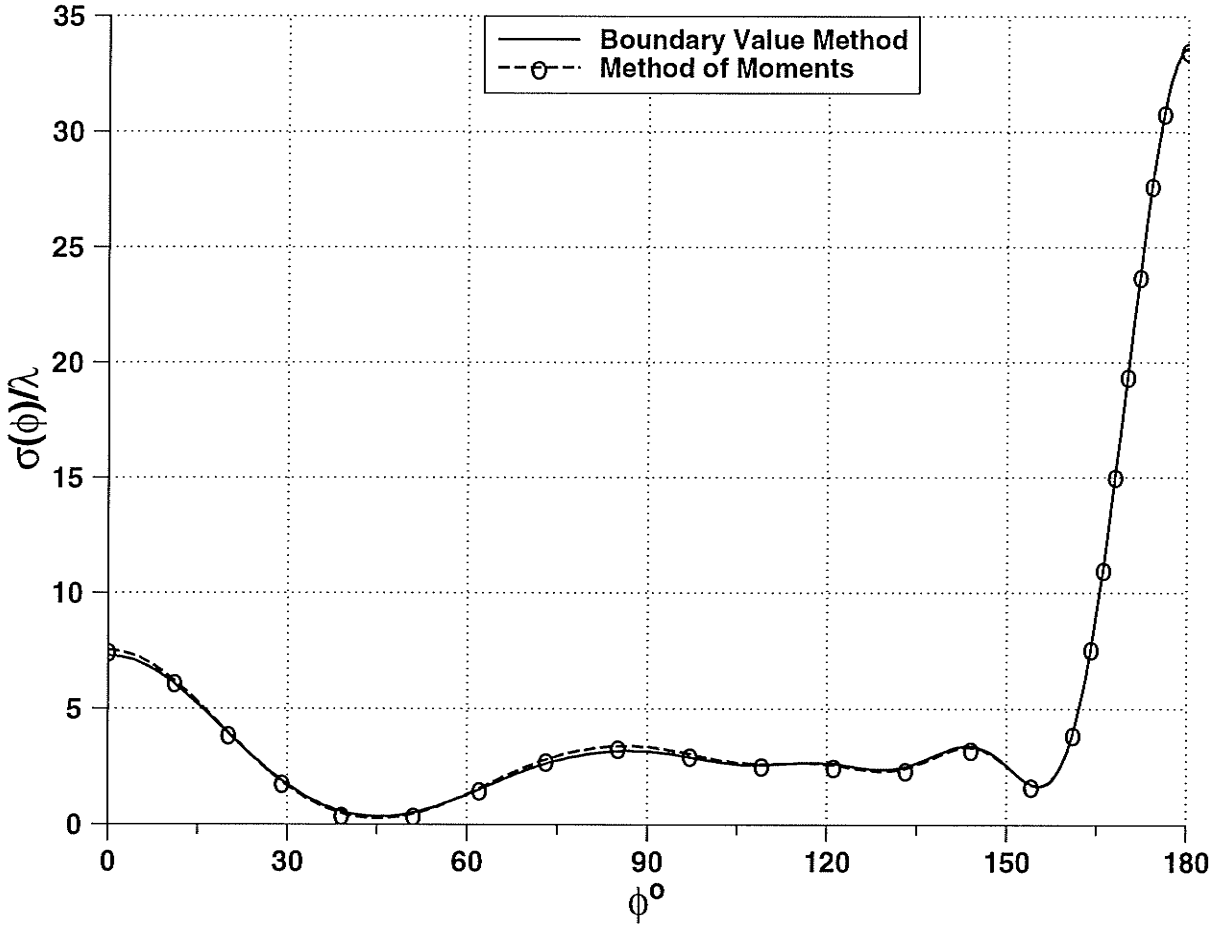

Figure 4.16: Bistatic scattering width with $ka = 2\pi$, $\varepsilon_r = 7$, $\phi_i = 0^o$, $\alpha = -25^o$ and $\beta = 25^o$.

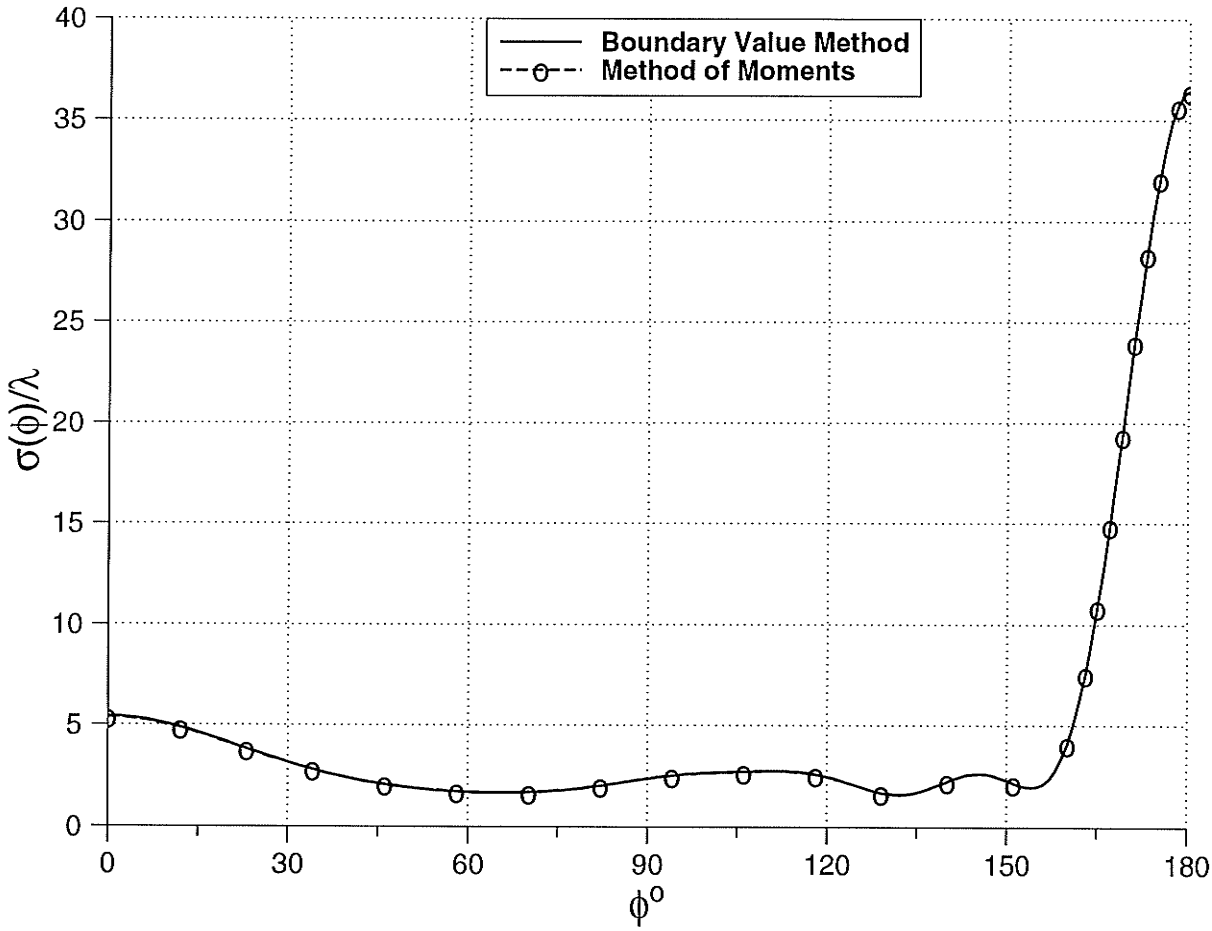

Figure 4.17: Bistatic scattering width with $ka = 2\pi$, $\varepsilon_r = 11$, $\phi_i = 0^o$, $\alpha = -25^o$ and $\beta = 25^o$.

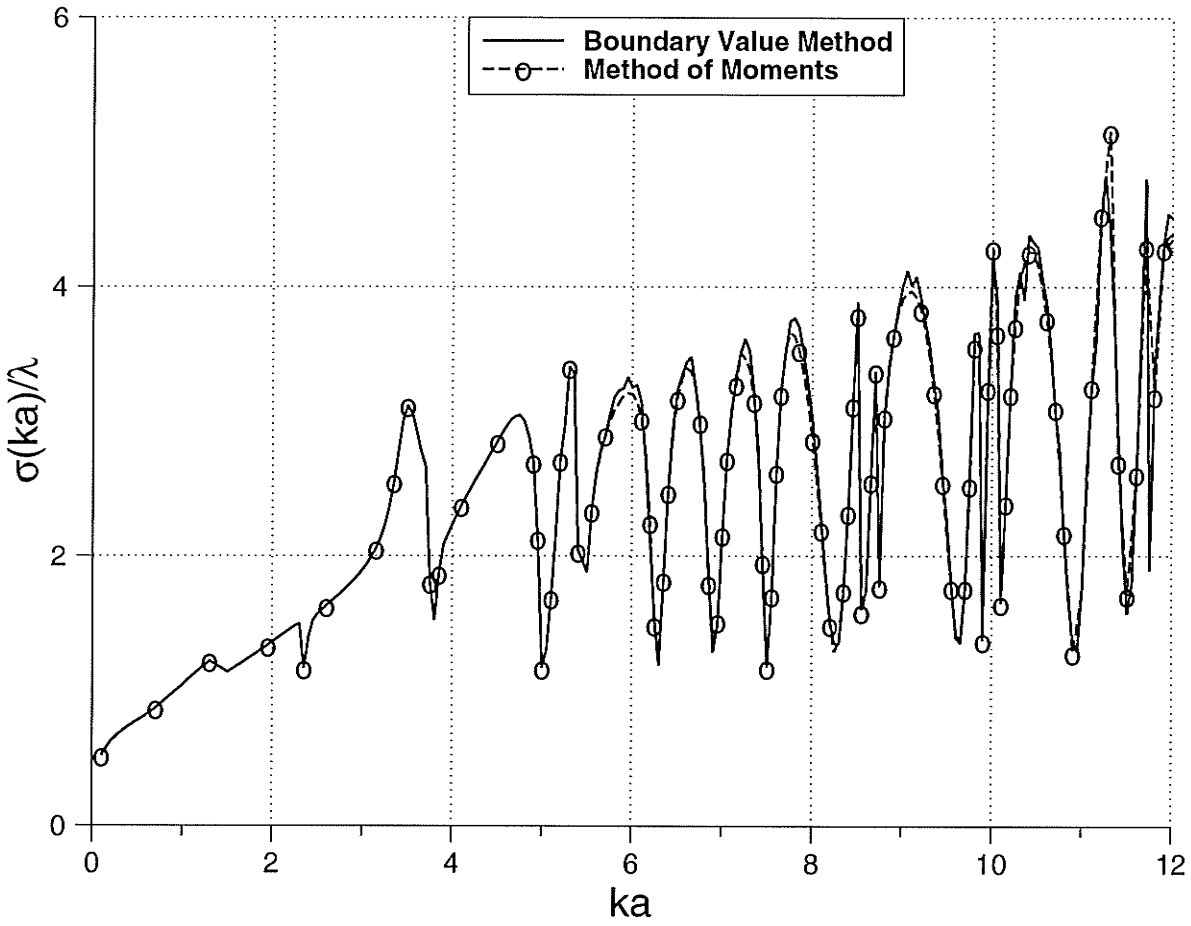

Figure 4.18: Back scattering width with $\varepsilon_r = 1$, $\phi_i = 0^o$, $\alpha = -5^o$ and $\beta = 5^o$.

CHAPTER 5

RESULTS AND DISCUSSION FOR THE MULTI-SLOT CASE

In this chapter numerical results for the multi-slot problem is presented. With knowledge of the expansion field coefficients a_{q_j} and b_{q_j} from (3.19) and (3.29), respectively, the unknown expansion field coefficients can be found as discussed in Chapter 3. The surface and far fields can be determined and compared for the two proposed methods. The bistatic scattering width can be found using (4.1).

5.1 Comparison Results

To obtain numerical results, the cylinder is taken to have an electrical radius of $ka = 2\pi$. To examine the accuracy of the solution over the boundary region, the tangential component of the total electric field (E_z) was computed using (3.1) and (3.2) with $\phi_i = 0^o$, and $\varepsilon_r = 1$ for two different cases. Fig.5.1 shows the results of the total tangential electric field for two equal slot angles where $\alpha_1 = -5^o, \beta_1 = 5^o, \alpha_2 = 175^o$ and $\beta_2 = 185^o$. Fig. (5.2) shows the same result, but for two different slot angles,*i.e.* $\alpha_1 = -25^o, \beta_1 = 25^o, \alpha_2 = 175^o$ and $\beta_2 = 185^o$. The two results show good agreement between the two methods, and also confirm that

the total tangential electric field vanishes at the conducting surface. Moreover, (3.1) and (3.2) give the same results for the total tangential electric field. Fig 5.3 shows a comparison between a complete conducting cylinder, and a two-slots cylinder where $\varepsilon_r = \infty$ and μ_r approaches 0, $\alpha_1 = -25^o$, $\beta_1 = 25^o$, $\alpha_2 = 155^o$, $\beta_2 = 205^o$ and $\phi_i = 0^o$. The results show complete agreement between the exact solution and the two proposed methods.

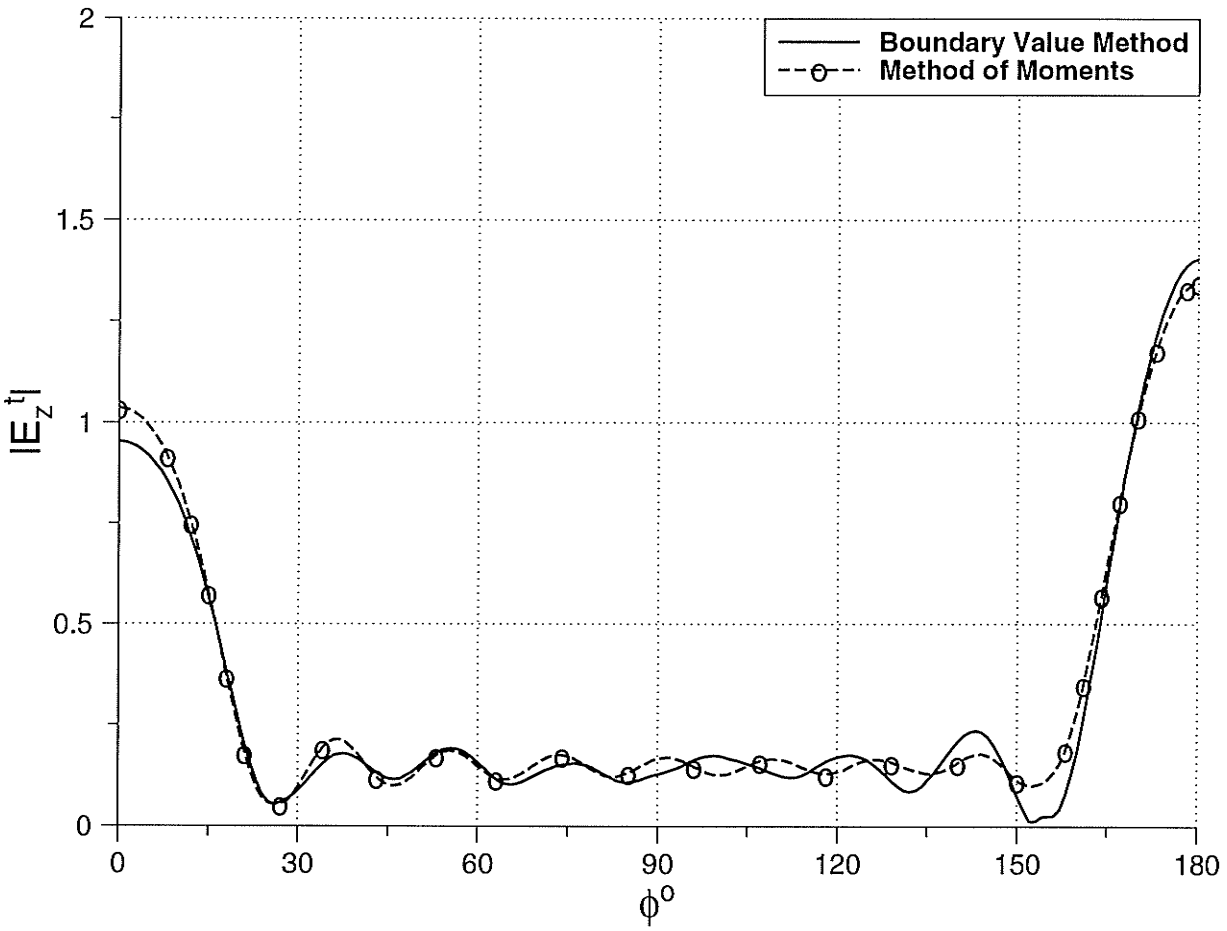

Figure 5.1: Total tangential electric field of a two slots cylinder with $ka = 2\pi$, $\varepsilon_r = 1$, $\phi_i = 0^o$, $\alpha_1 = -5^o$, $\beta_1 = 5^o$, $\alpha_2 = 175^o$ and $\beta_2 = 185^o$.

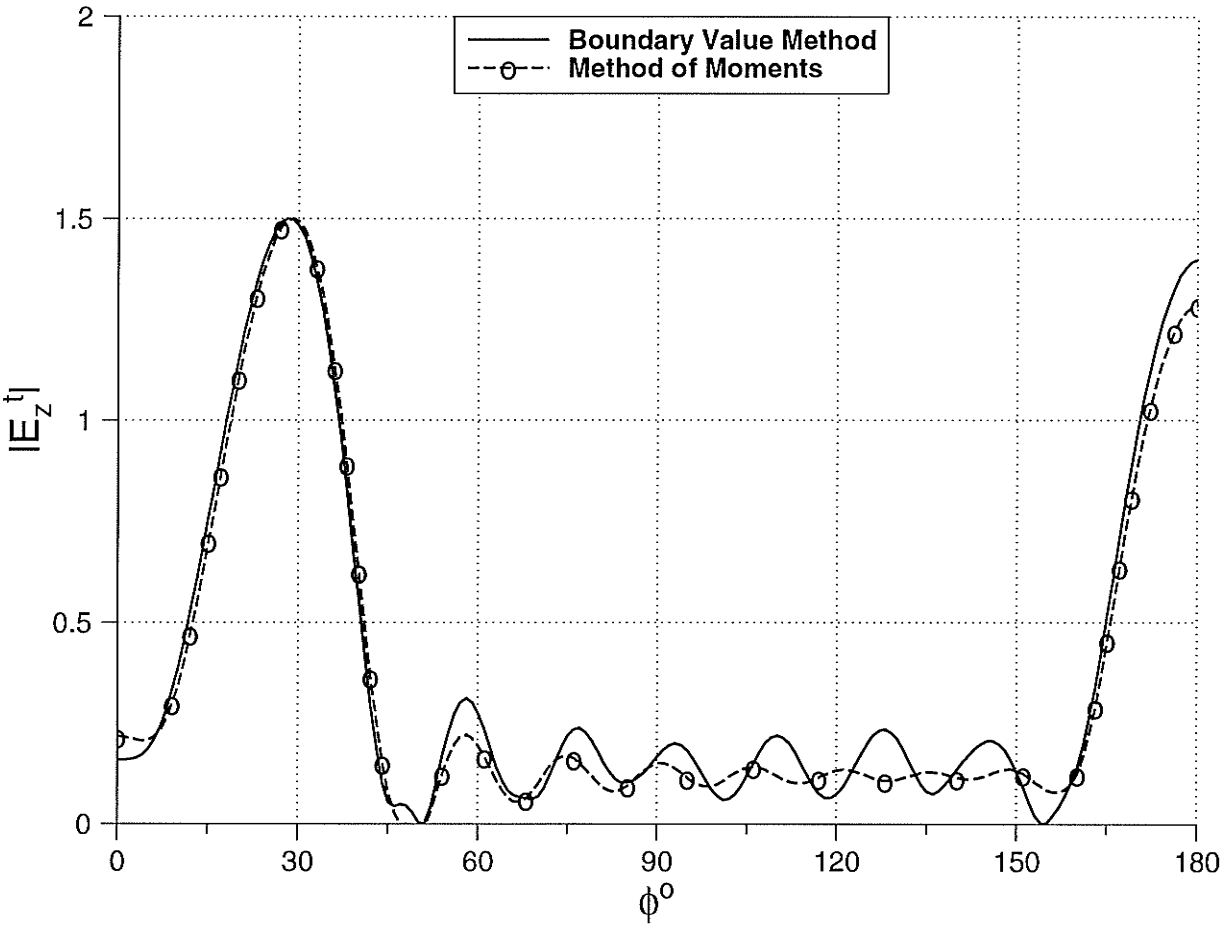

Figure 5.2: Total tangential electric field of a two slots cylinder with $ka = 2\pi$, $\varepsilon_r = 1$, $\phi_i = 0^o$, $\alpha_1 = -25^o$, $\beta_1 = 25^o$, $\alpha_2 = 175^o$ and $\beta_2 = 185^o$.

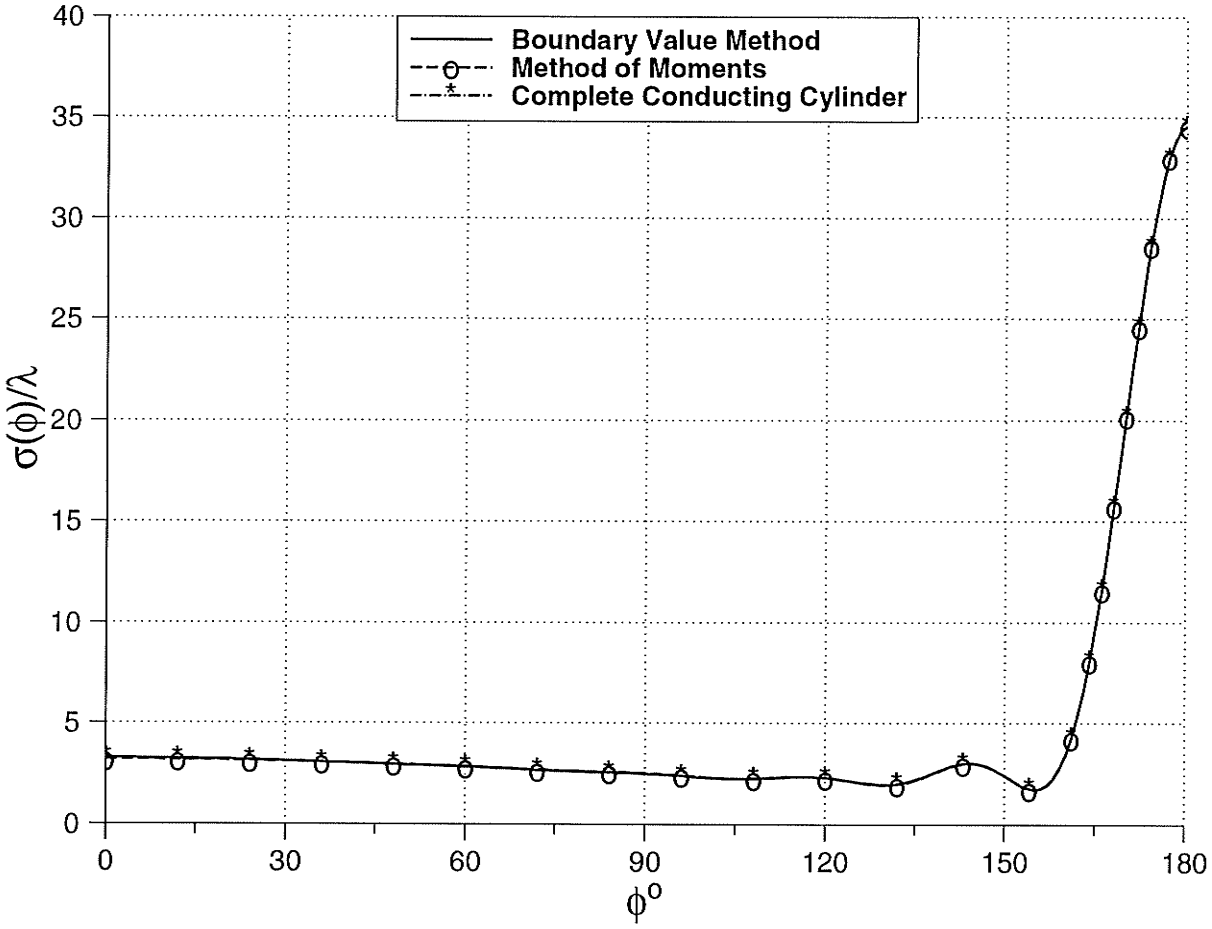

Figure 5.3: Comparison of bistatic scattering width for a complete conducting cylinder and a cylinder with two slots, $\varepsilon_r = \infty$, $\phi_i = 0^o$, $\alpha_1 = -25^o$ and $\beta_1 = 25^o$ $\alpha_2 = 155^o$ and $\beta_2 = 205^o$.

5.2 Results for Far Scattered Field

Figs. (5.4–5.7) show the results of the far scattered field for two slots *i.e.* ($\alpha_1 = -25^o, \beta_1 = 25^o, \alpha_2 = 175^o$ and $\beta_2 = 185^o$) and an arbitrary angles of incidence equal to $\phi_i = 0^o, 90^o, 180^o$ and 270^o, respectively. It can be concluded that the maximum scattered field occurs in the forward direction, and the direction of incidence affects the strength of the maximum scattered field, the number of oscillations and their strength. The far scattered fields for different slot angles and different slot positions are given in Figs. (5.8–5.9), where it can be concluded that as the slot size increases the forward scattered field decreases while the side lobe level increases. The back scattering width for a two-slot cylinder, where $\alpha_1 = -5^o$, $\beta_1 = 5^o, \alpha_2 = 175^o, \beta_2 = 185^o$ and $\varepsilon_r = 1$, is given in Fig. (5.10), and due to symmetry, is presented over the range from 0^o to 90^o showing that the maximum back scattering width occurs in between the two slots.

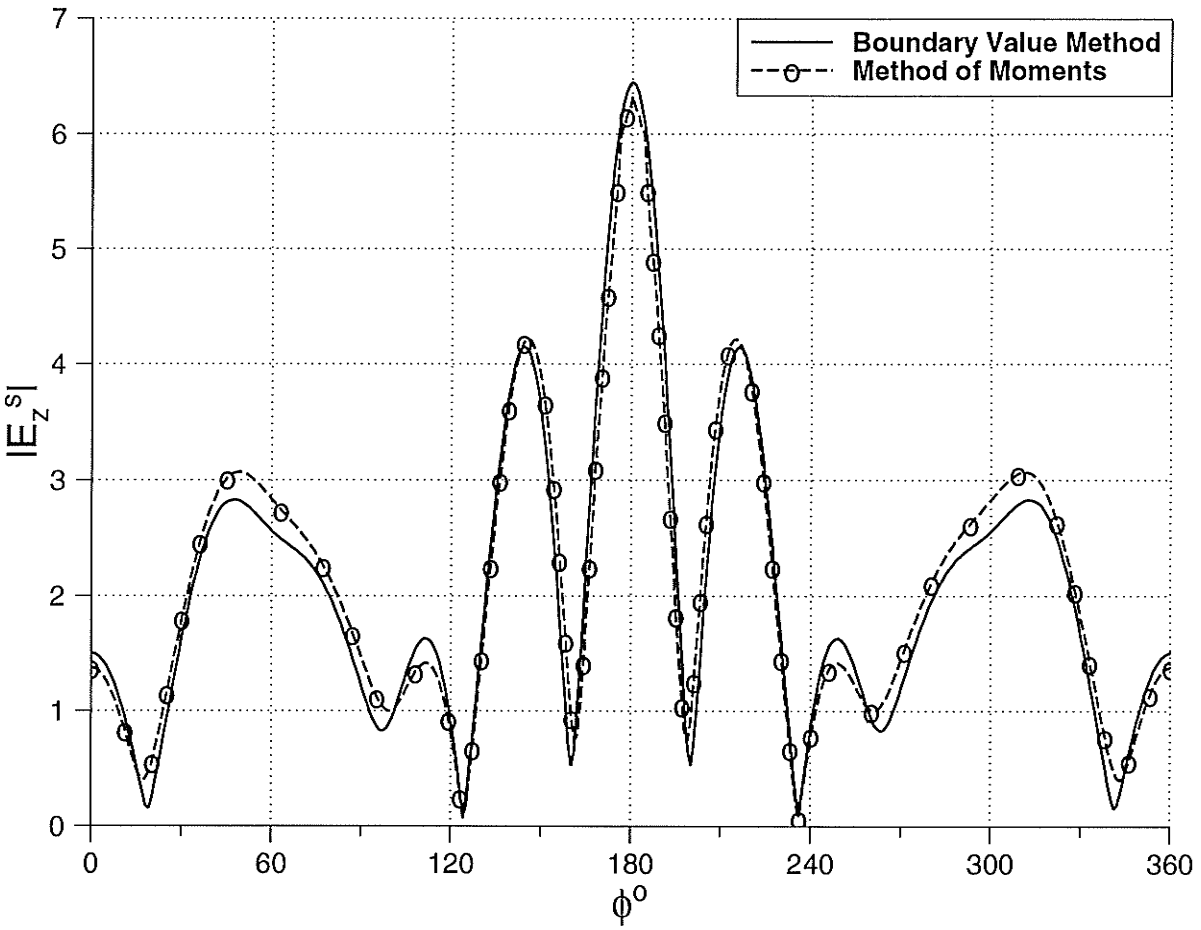

Figure 5.4: Far scattered field of a two slots cylinder with $ka = 2\pi$, $\varepsilon_r = 1$, $\phi_i = 0^o$, $\alpha_1 = -25^o$, $\beta_1 = 25^o$, $\alpha_2 = 175^o$ and $\beta_2 = 185^o$.

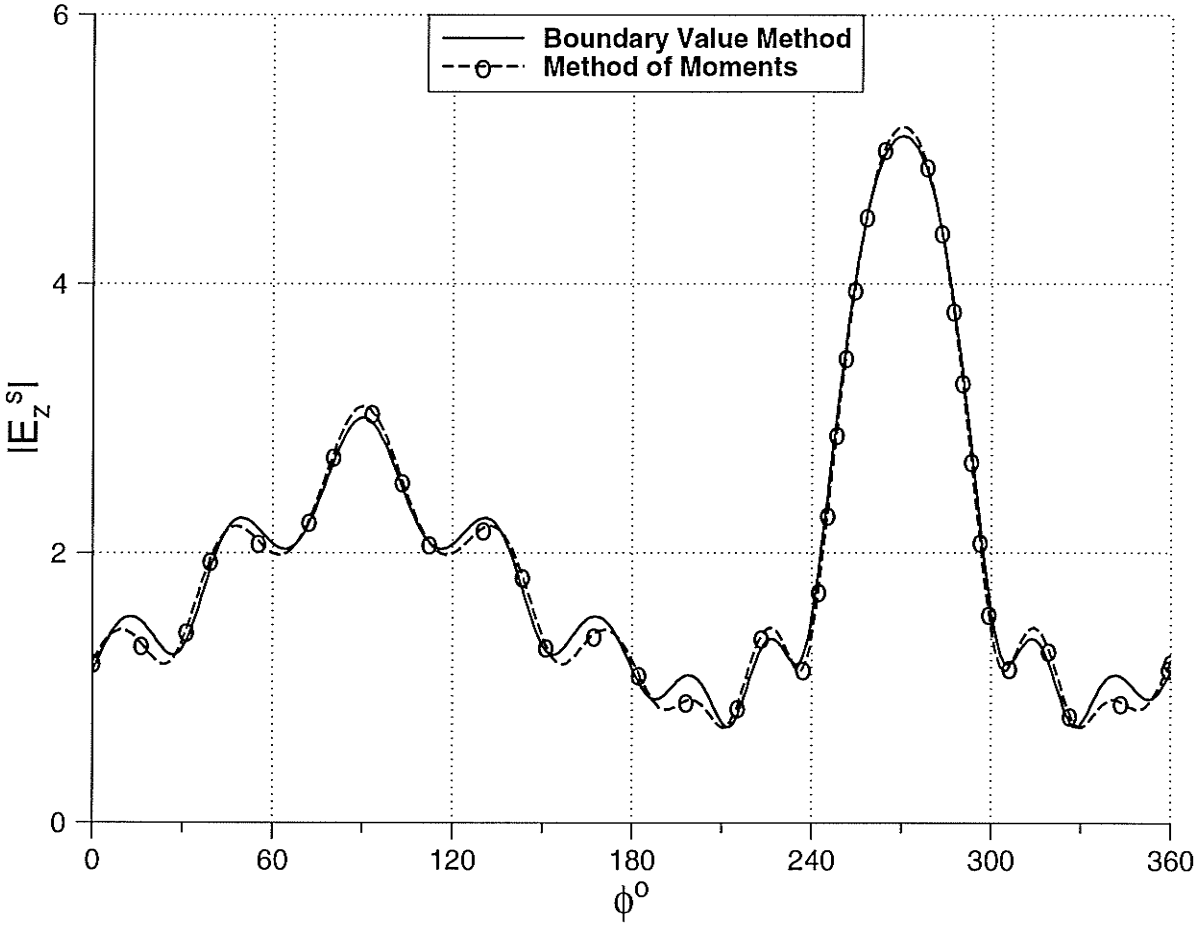

Figure 5.5: Far scattered field of a two slots cylinder with $ka = 2\pi$, $\varepsilon_r = 1$, $\phi_i = 90^o$, $\alpha_1 = -25^o$, $\beta_1 = 25^o$, $\alpha_2 = 175^o$ and $\beta_2 = 185^o$.

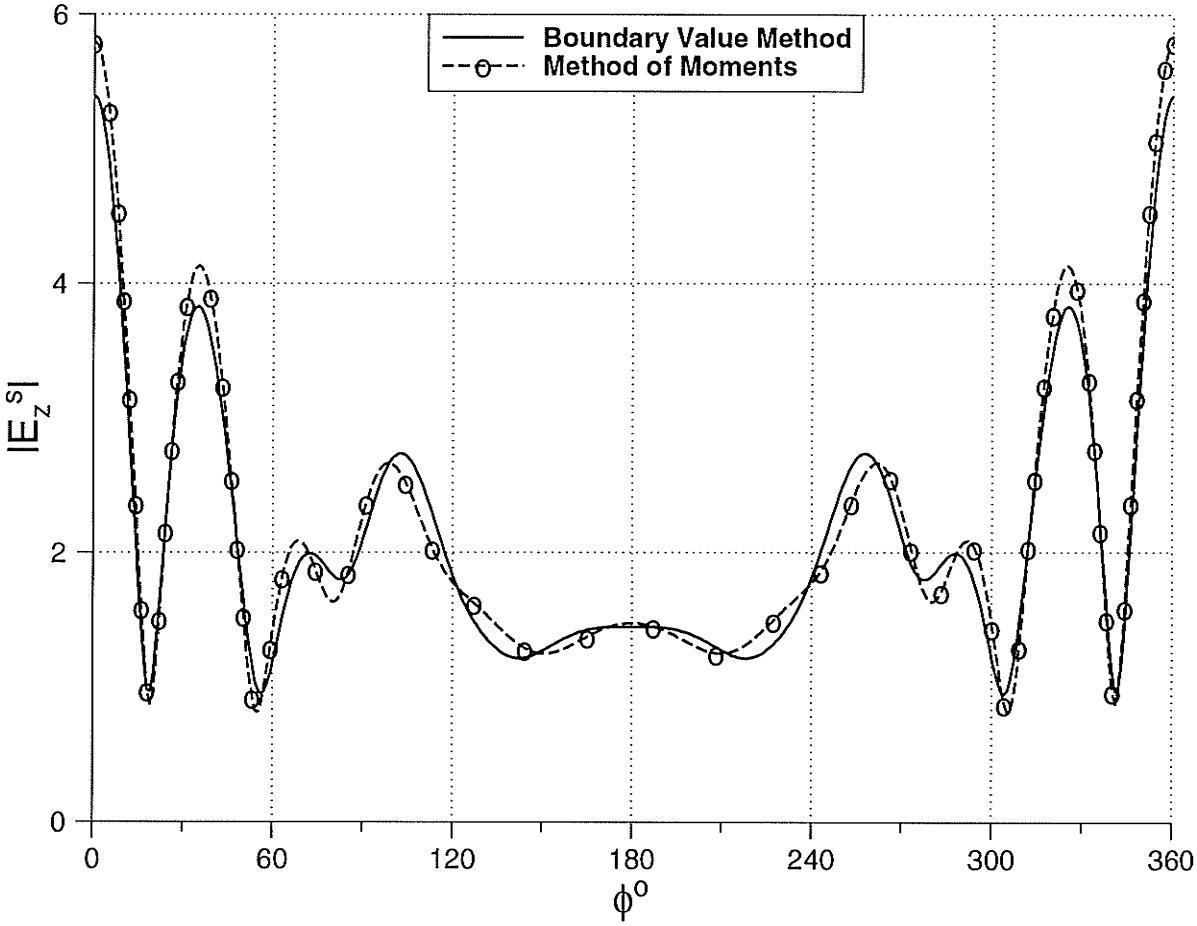

Figure 5.6: Far scattered field of a two slots cylinder with $ka = 2\pi$, $\varepsilon_r = 1$, $\phi_i = 180^o$, $\alpha_1 = -25^o$, $\beta_1 = 25^o$, $\alpha_2 = 175^o$ and $\beta_2 = 185^o$.

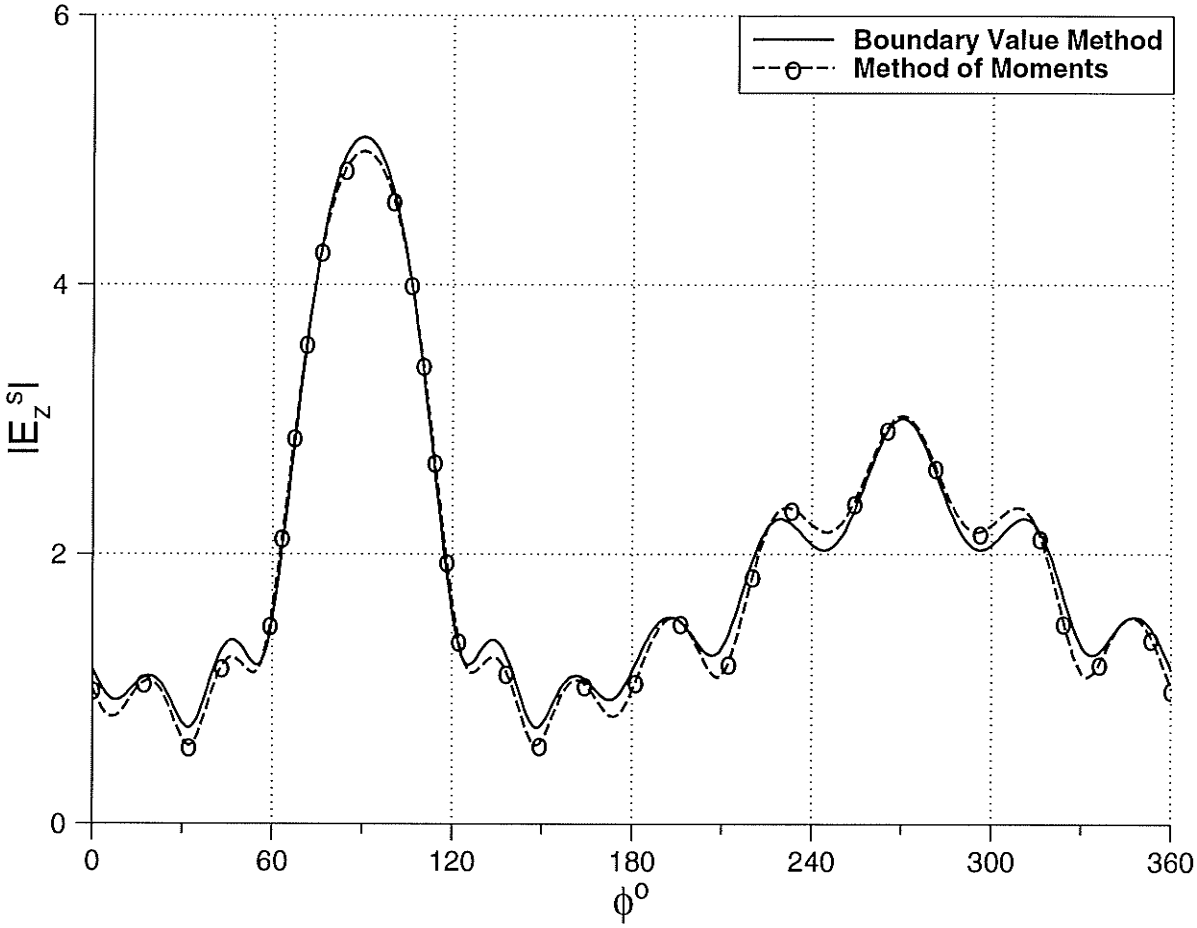

Figure 5.7: Far scattered field of a two slots cylinder with $ka = 2\pi$, $\varepsilon_r = 1$, $\phi_i = 270^o$, $\alpha_1 = -25^o$, $\beta_1 = 25^o$, $\alpha_2 = 175^o$ and $\beta_2 = 185^o$.

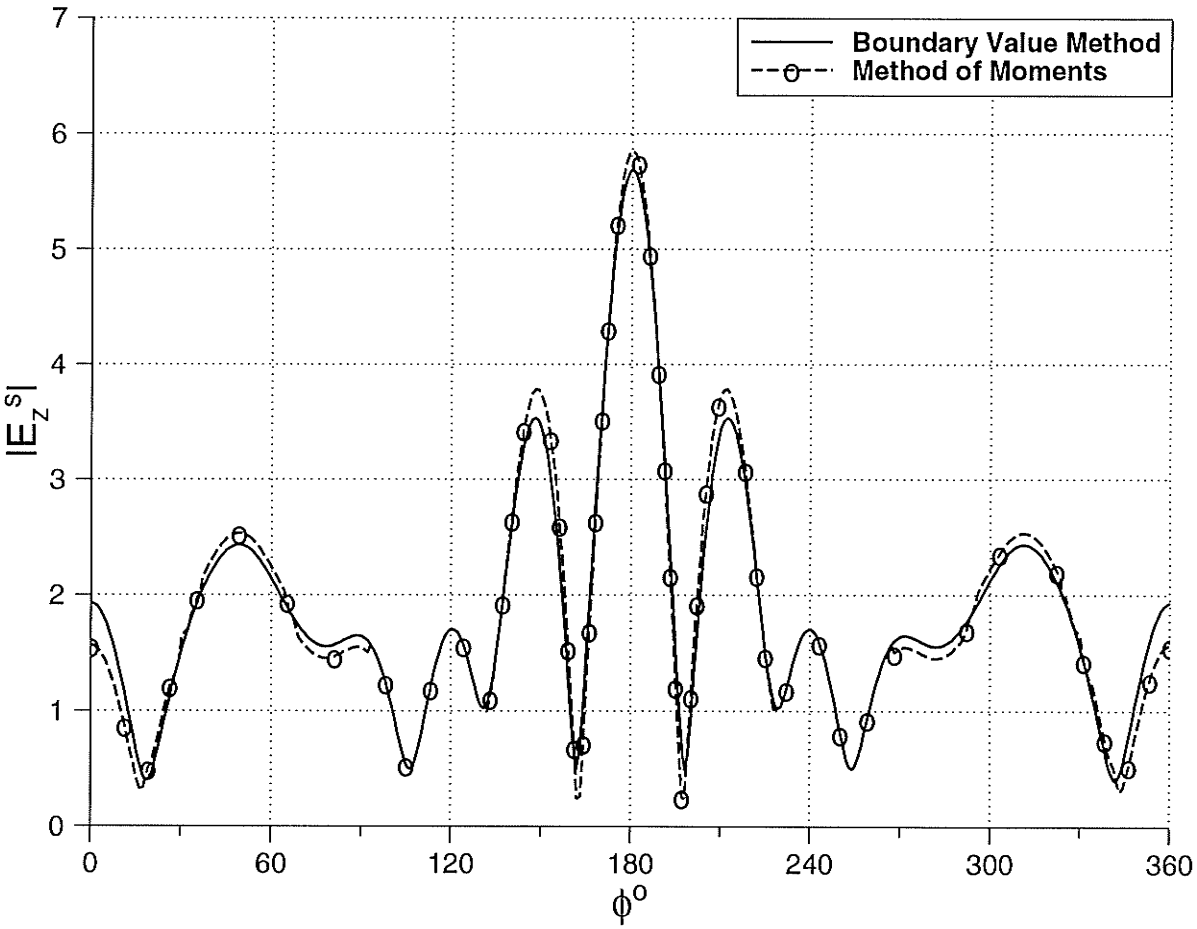

Figure 5.8: Far scattered field of a two slots cylinder with $ka = 2\pi$, $\varepsilon_r = 1$, $\phi_i = 0^o$, $\alpha_1 = -25^o$, $\beta_1 = 25^o$, $\alpha_2 = 205^o$ and $\beta_2 = 155^o$.

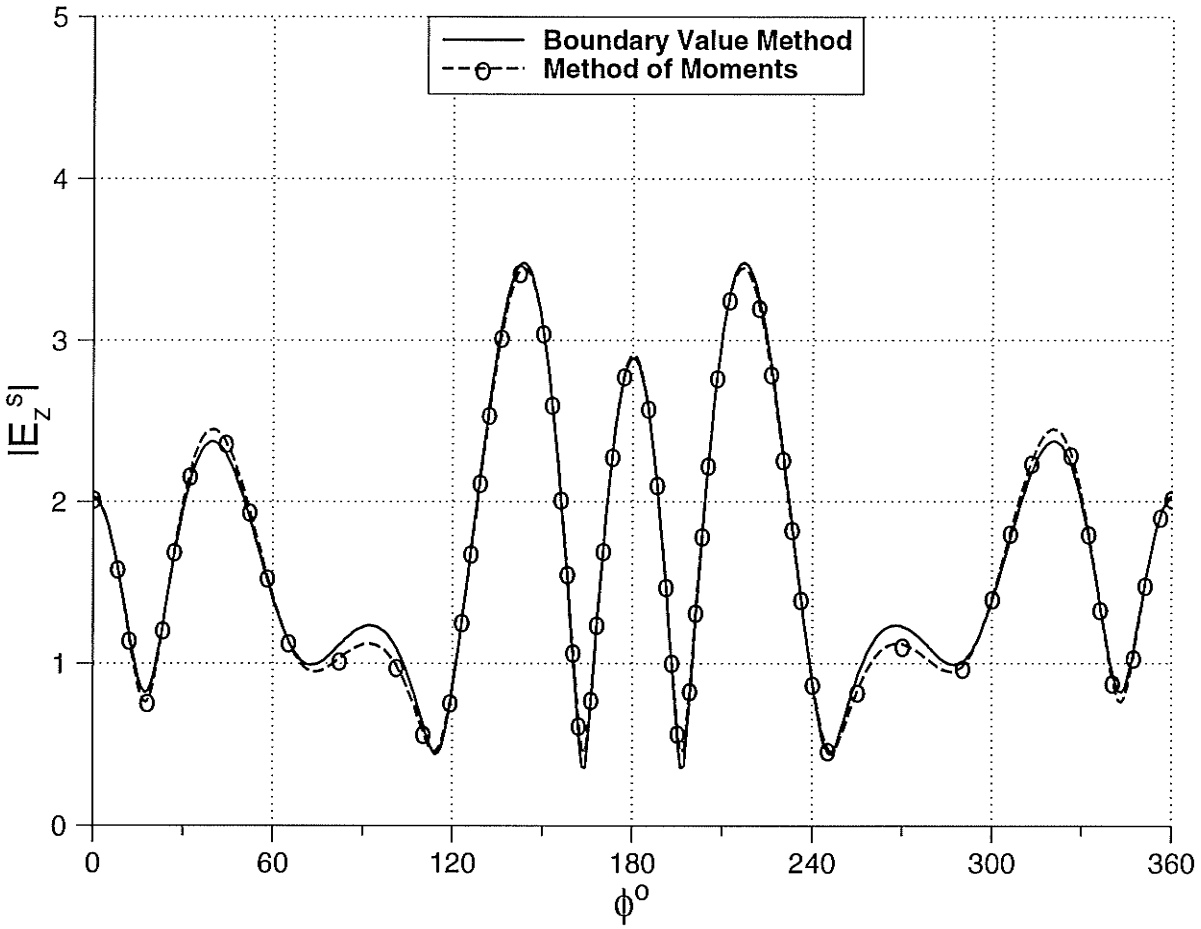

Figure 5.9: Far scattered field of a two slots cylinder with $ka = 2\pi$, $\varepsilon_r = 1$, $\phi_i = 0^o$, $\alpha_1 = -90^o$, $\beta_1 = 90^o$, $\alpha_2 = 175^o$ and $\beta_2 = 185^o$.

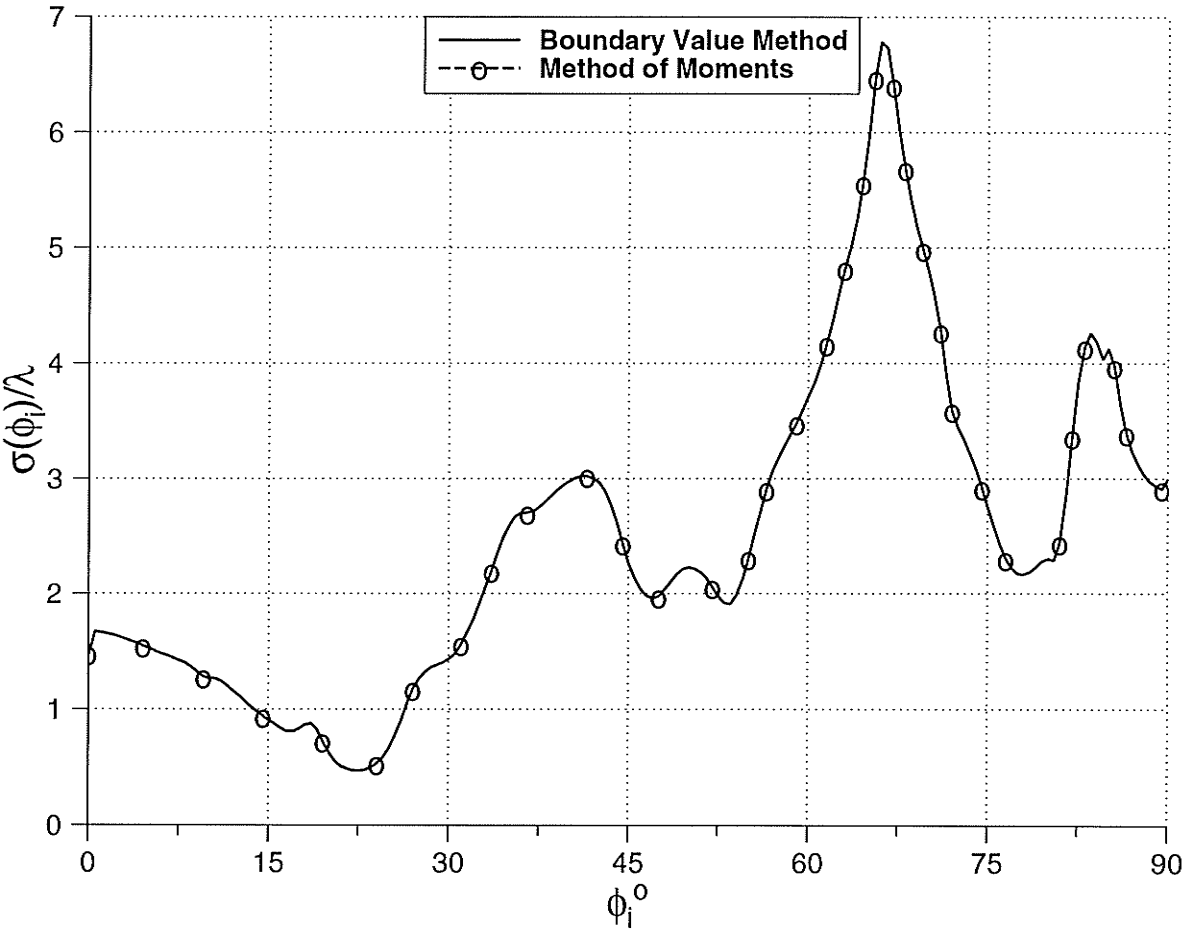

Figure 5.10: Back scattering width of a two slots cylinder with $ka = 2\pi$, $\varepsilon_r = 1$, $\alpha_1 = -5^o$, $\beta_1 = 5^o$, $\alpha_2 = 175^o$ and $\beta_2 = 185^o$.

5.3 Results for Bistatic Scattering Width

The results for the bistatic scattering width for different slot angles are shown in Figs. (5.11–5.13). It is clear that as the size of the forward slot (facing the incident wave) increases, the forward bistatic scattering width increases. On the other hand, as the back slot (180^o away from the incidence direction) increases in size, the forward bistatic scattering width decreases. However, increasing the size of the slots results in an increase in the number of oscillations and their amplitude.

The effects of loading the inner region of the cylinder with different dielectric materials for a cylinder with different slot angles are shown in Figs. (5.14–5.16). It can be observed that the loading increases the forward bistatic scattering width and also reduces and smooths the oscillations elsewhere. Finally Fig. (5.17) shows the results for the back scattering width with respect to the electrical radius ka of a cylinder with two identical slots of 10^o *i.e.* ($\alpha_1 = -5^o, \beta_1 = 5^o, \alpha_2 = 175^o$ and $\beta_2 = 185^o$), $\varepsilon_r = 1$ and $\phi_i = 0^o$, from which it is clear that as ka increases the back scattering width increases.

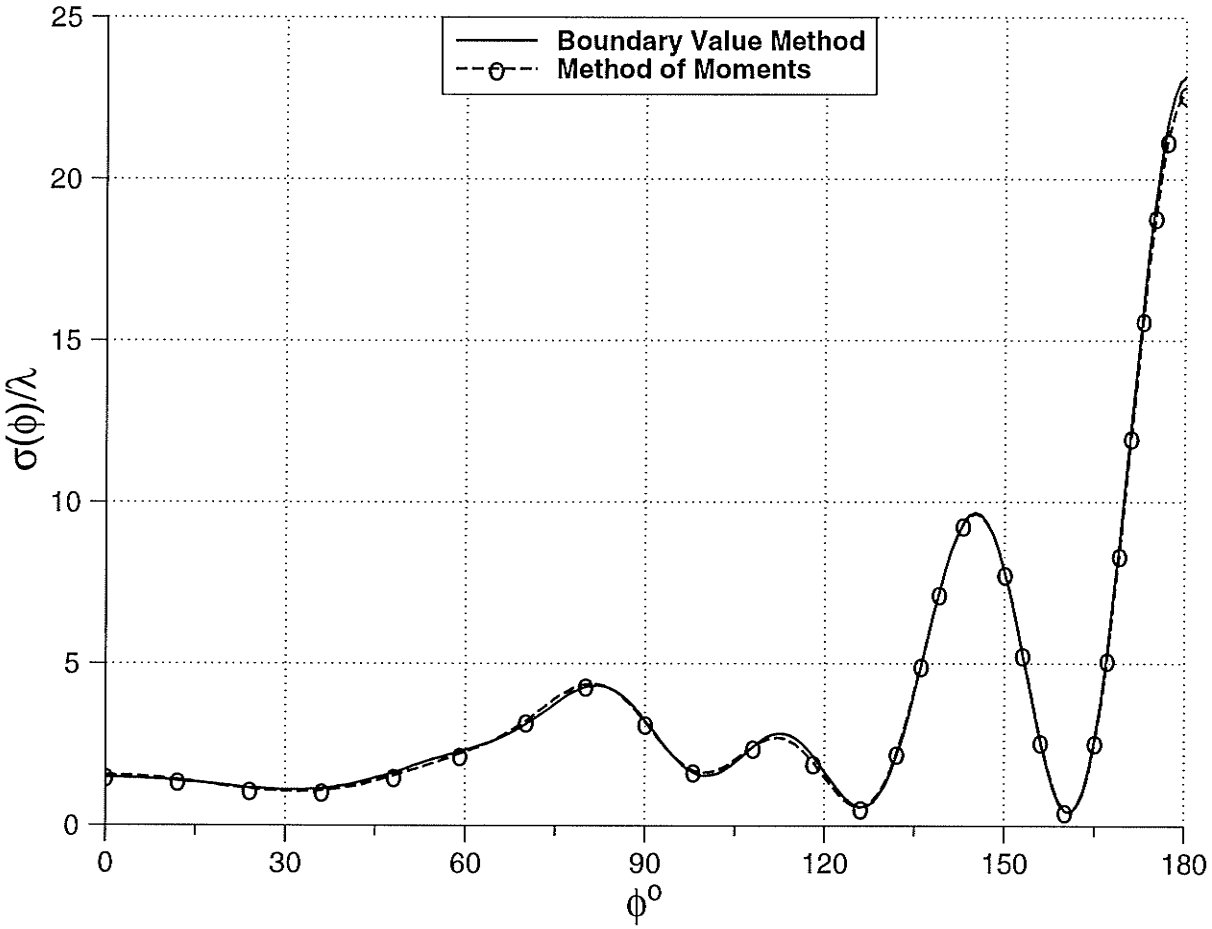

Figure 5.11: Bistatic scattering width of a two slots cylinder with $ka = 2\pi$, $\varepsilon_r = 1$, $\phi_i = 0^o$, $\alpha_1 = -5^o$, $\beta_1 = 5^o$, $\alpha_2 = 175^o$ and $\beta_2 = 185^o$.

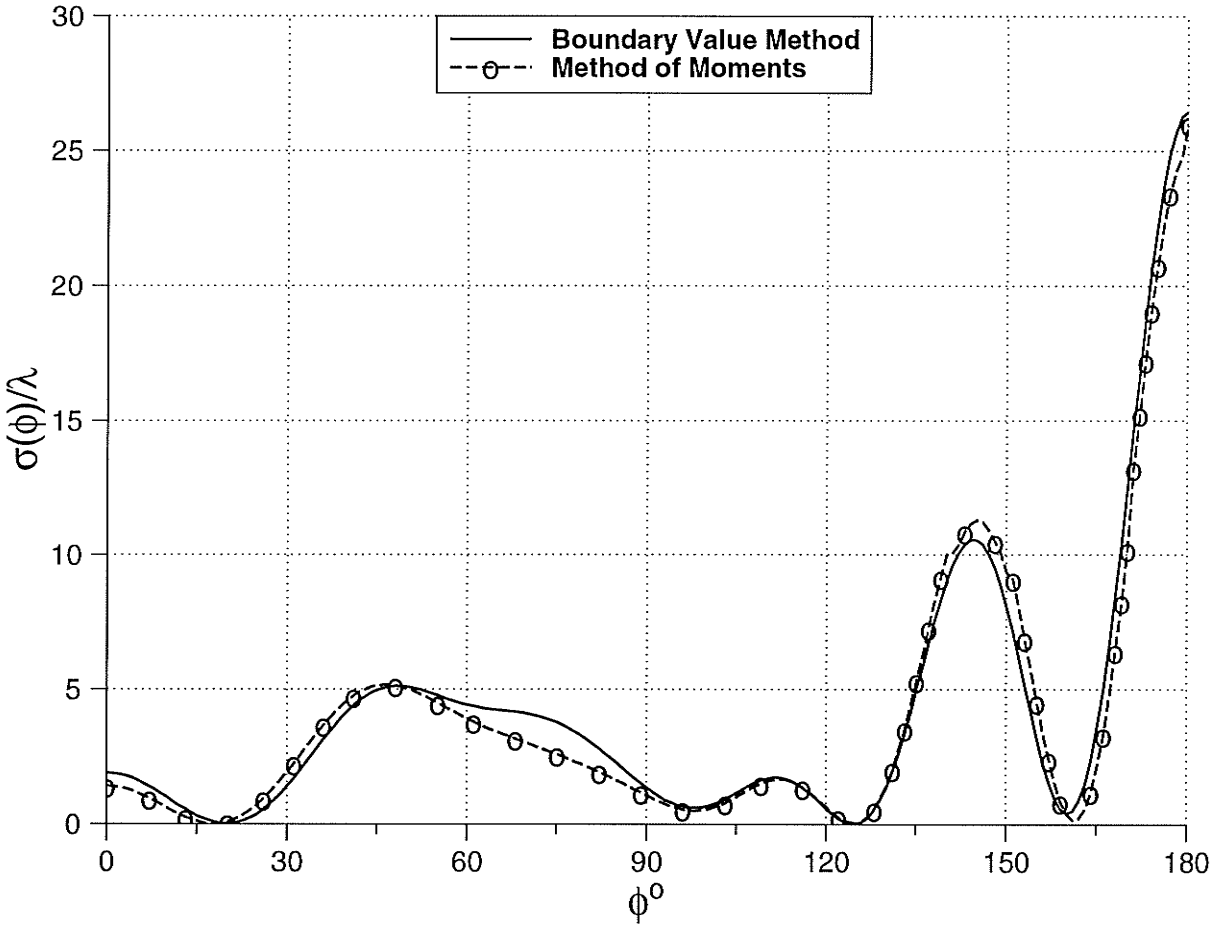

Figure 5.12: Bistatic scattering width of a two slots cylinder with $ka = 2\pi$, $\varepsilon_r = 1$, $\phi_i = 0^o$, $\alpha_1 = -25^o$, $\beta_1 = 25^o$, $\alpha_2 = 175^o$ and $\beta_2 = 185^o$.

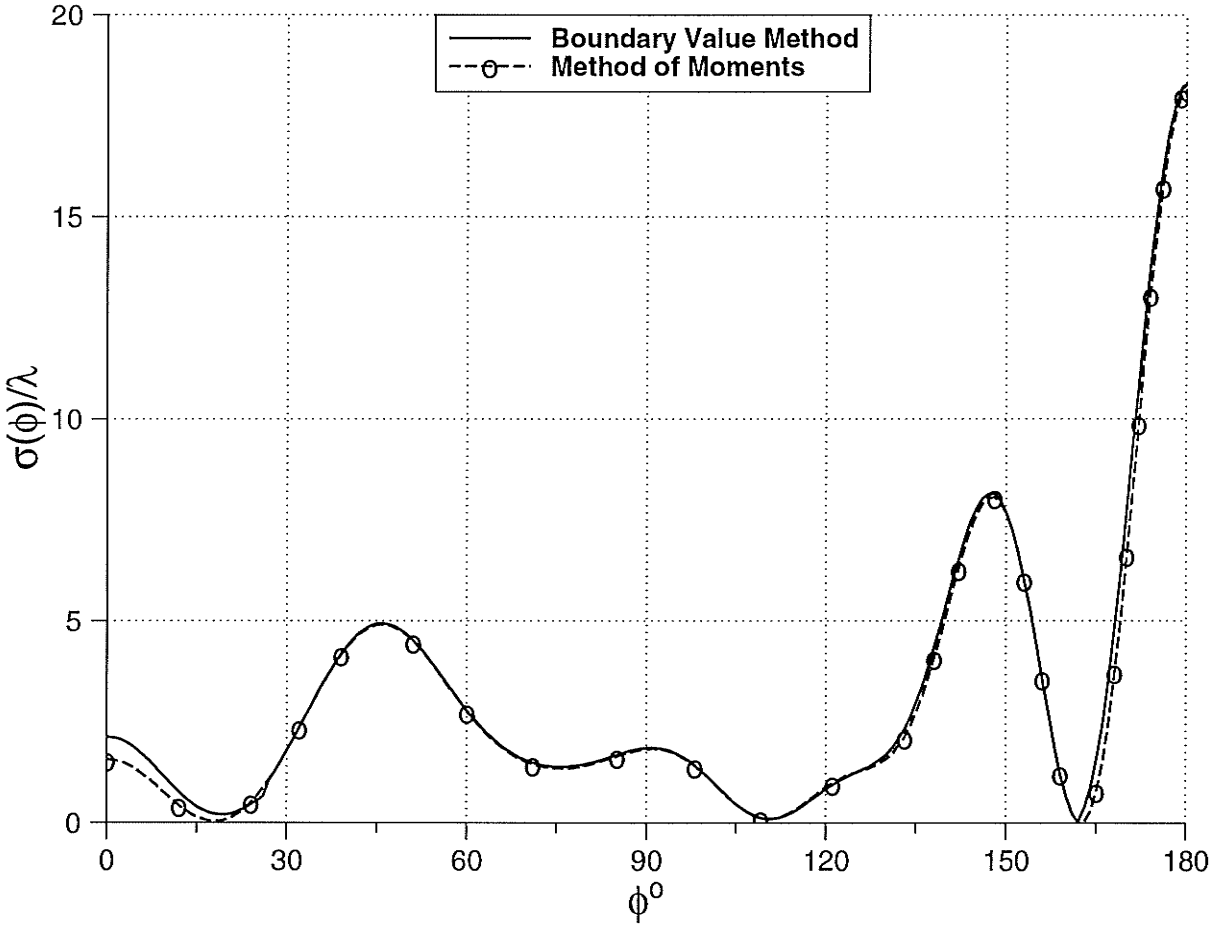

Figure 5.13: Bistatic scattering width of a two slots cylinder with $ka = 2\pi$, $\varepsilon_r = 1$, $\phi_i = 0^o$, $\alpha_1 = -25^o$, $\beta_1 = 25^o$, $\alpha_2 = 155^o$ and $\beta_2 = 205^o$.

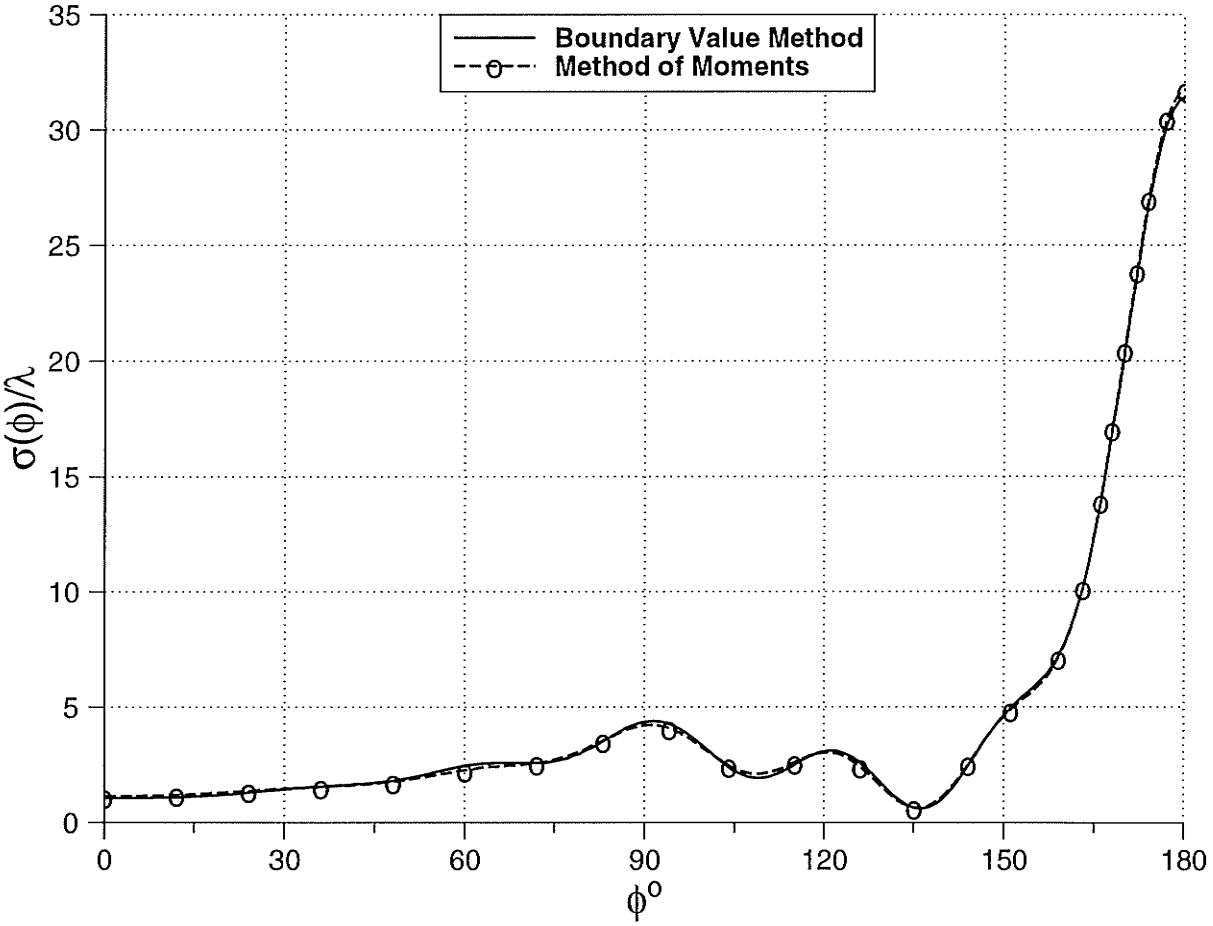

Figure 5.14: Bistatic scattering width of a two slots cylinder with $ka = 2\pi$, $\varepsilon_r = 10$, $\phi_i = 0^o$, $\alpha_1 = -5^o$, $\beta_1 = 5^o$, $\alpha_2 = 175^o$ and $\beta_2 = 185^o$.

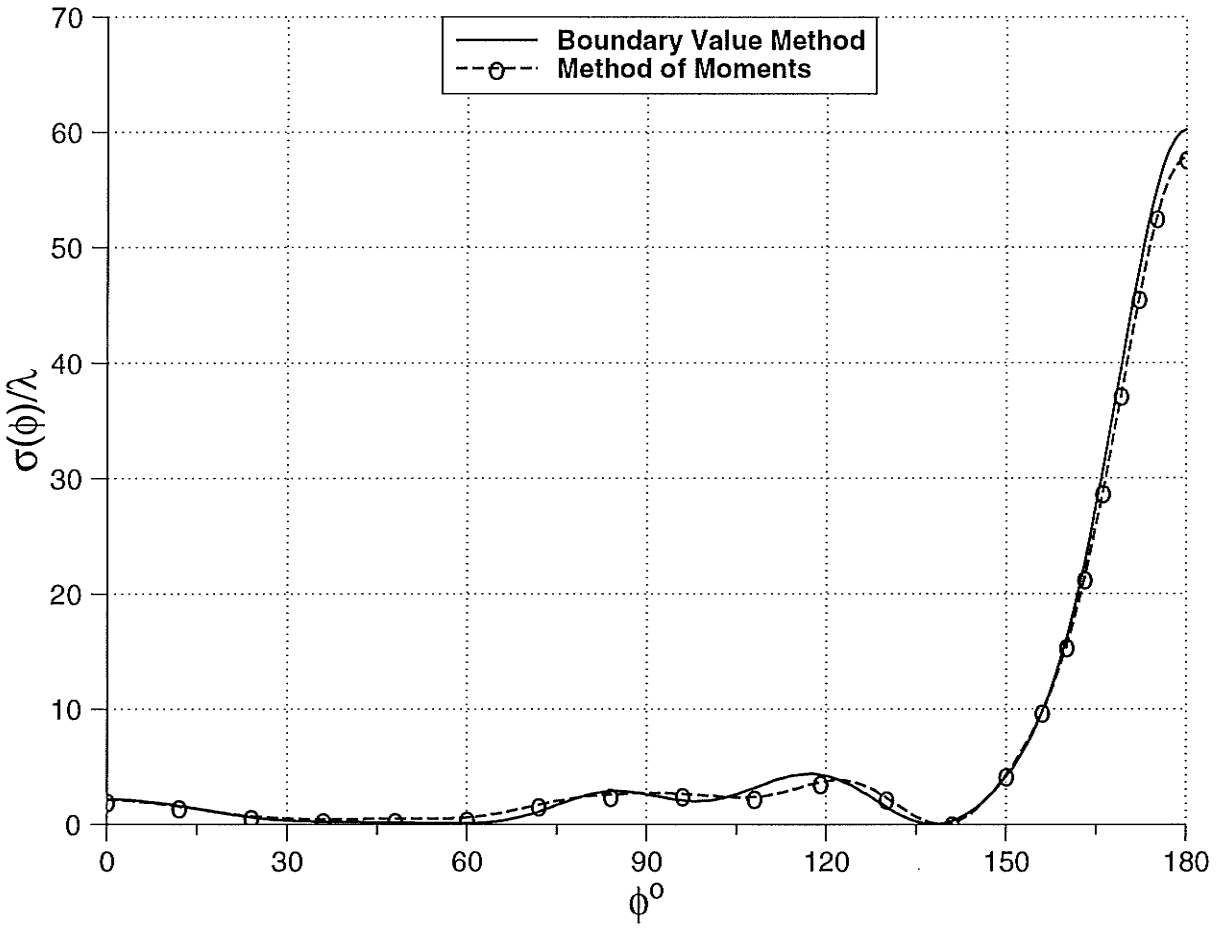

Figure 5.15: Bistatic scattering width of a two slots cylinder with $ka = 2\pi$, $\varepsilon_r = 3$, $\phi_i = 0^o$, $\alpha_1 = -25^o$, $\beta_1 = 25^o$, $\alpha_2 = 155^o$ and $\beta_2 = 205^o$.

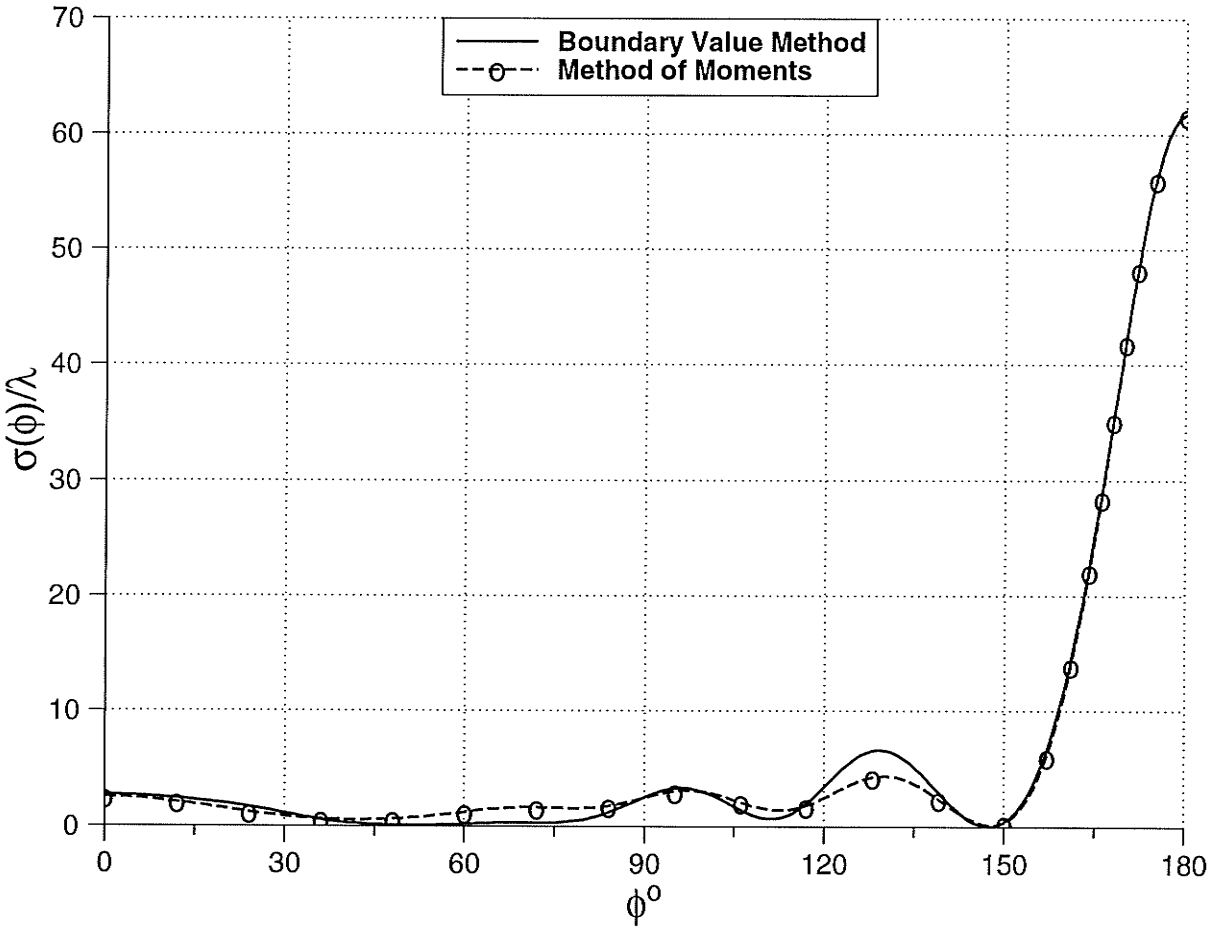

Figure 5.16: Bistatic scattering width of a two slots cylinder with $ka = 2\pi$, $\varepsilon_r = 11$, $\phi_i = 0^o$, $\alpha_1 = -25^o$, $\beta_1 = 25^o$, $\alpha_2 = 155^o$ and $\beta_2 = 205^o$.

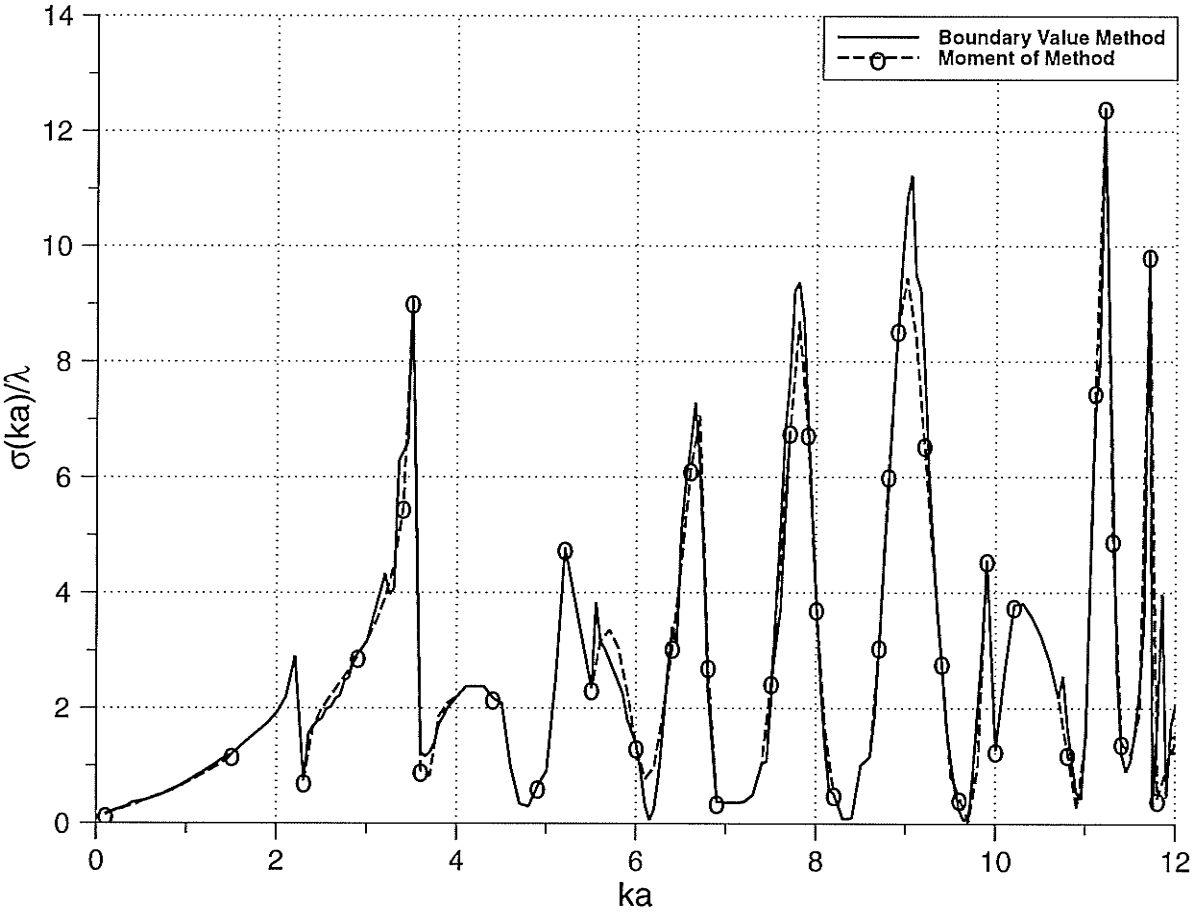

Figure 5.17: Back scattering width with $\varepsilon_r = 1, \phi_i = 0^o, \alpha_1 = -5^o$, $\beta_1 = 5^o$, $\alpha_2 = 175^o$ and $\beta_2 = 185^o$

CHAPTER 6

CONCLUSIONS AND RECOMMENDATIONS

The problem of scattering by a perfectly conducting circular multi-slotted cylinder has been investigated in this thesis. In Chapter 2 the discussion was restricted to a single slot cylinder. The analysis was carried out using the boundary value method. The aperture field integral equation method was introduced and the results were compared numerically with the boundary value method. The agreement between the two methods for the surface tangential electric field, the far scattered field, the back scattering width and the bistatic scattering width was excellent in all cases studied. The accuracy of the solution was obtained by examining the solution over the boundary region. The surface tangential electric field was computed using the two methods, and the results confirmed that the total tangential electric field vanishes over the conducting surface. Also the solution was examined for the case where ε_r approaches ∞ and μ_r approaches 0. The results were in a very good agreement with the exact solution of the complete conducting cylinder. It should be pointed out that the accuracy and the convergence of the solution are highly dependent on the slot size, the position of the slot with respect to the incidence field, the radius of the cylinder and the dielectric media in the inner region.

In Chapter 3, the solution was extended to include a multi-slot cylinder. Meth-

ods of analysis used here were the same as those used in Chapter 2. The multi-slot problem required the need of N-system of matrix equations according to the number of slots. The investigation was limited to two-slot cylinder and the results were obtained regarding the surface tangential electric field, the far scattered field, the back scattering width and the bistatic scattering width. Similar to the case of the single-slot, the accuracy of the solution was obtained by examining the solution over the boundary region. Moreover, the solution was varified also with the complete conducting cylinder by taking $\varepsilon_r = \infty$ and mu_r approaches 0. The agreement between the two methods was excellent in all cases studied. A point worth mentioning is that the accuracy and convergence of the solution is dependent on the factors mentioned above for the single-slot cylinder. In addition the spacing between the slots and the number of slots has a great effect on the behavior of the scattered field.

Although the solution up to two slots was investigated, it is obviously of interest to extend the effort to three slots and more. Another potential study is to investigate an optimum design, taking into account the cylinder size relative to the wave length, number, size and spacing between the slots to maximize or minimize the scattering width. Finally, the work can be extended to loading the interior and the exterior regions of the cylinder with dielectric multi-layers

REFERENCES

REFERENCES

[1] G. Hasserjian and A. Ishimaru. Current induced on the surface of conducting circular cylinder by a slot. *Radio Propagat.*, vol. 66 D, no. 3, pp. 335–365, 1962.

[2] Andrejs Olte. Radiation of an elementary cylinder antenna through a slotted enclosure. *IEEE Trans. Antennas Propagat.*, vol. AP-13, no. 5, pp. 691–703, Sept. 1965.

[3] J. Richmond and M. Gilreath. Flush-mounted dielectric-loaded axial slot on circular cylinder. *IEEE Trans. Antennas Propagat.*, vol. AP-23, no. 3, pp. 348–351, May 1975.

[4] W. A. Johnson and R. W. Ziolkowski. The scattering of an H-polarized plane wave from an axial slotted infinite cylinder: a daul series approach. *Radio sci.*, vol. 19, no. 1, pp. 275–291, Jan. 1984.

[5] R. W. Ziolkowski. N-series problems and the coupling of electromagnetic waves to apertures: A Rieman-Hilbert approach. *SIAM J. Math. Anal.*, vol. 16, no. 2, March 1985.

[6] D. R. Rhodes. Theory of axially slitted circular and elliptic cylinder antenna. *J. Appl. Phys.*, vol. 21, pp. 1181–1188, Nov. 1950.

[7] P. M. Morse and H. Feshback. *Method of Theoretical Physics.* McGraw Hill, New York, 1953.

[8] Jeffrey A. Beren. Diffraction of an H-polarized electromagnetic wave by a circular cylinder with infinite axial slot. *IEEE trans. Antennas Propagat.*, vol. AP-31, no. 3, pp. 419–425, May 1983.

[9] C. A. Klein and R. Mittra. An application of the condition number concept to the solution of scattering problem in the presence of the interior resonant frequencies. *IEEE Trans. Antennas Probagat.*, vol. AP-23, no. 3, pp. 431–435, May 1975.

[10] T. B. A. Senior. Electromagnetic field penetration into a cylindrical cavity. Tech. Rep. IN 221, Air Force Weapons Lab. Interaction Notes, Jan. 1975.

[11] J. N. Bombardt and L. F. Libelo. S.E.R.A: V. surface current, tangential aperture electric field, and back-scattering cross section for axial slotted cylinder at normal, symmetric incidence. Tech. Rep. VSURFWPNCEN, NSWC/WOL/TR 75-39, White Oak Lab., April 1975.

[12] V. N. Koshpareand V. P. Shestopalov. Diffraction of a plane electromagnetic wave by a circular cylinder with a longitudinal slot. *Zh. Vychisl. Mat. Fiz.*, vol. 11, pp. 719–737, 1971.

[13] J. B. Billingsley and G. Sinclair. Numerical solution to electromagnetic scattering from srips, finite wedges, and notched circular cylinders. *Cand. J. of Phys.*, vol. 44, no. 12, pp. 3217–3225, December 1966.

[14] R. Ruppin and Yatom. Electromagnetic scattering from a coated notched cylinder. *Cand. J. of Phys.*, vol. 67, no. 6, pp. 587–591, June 1989.

[15] M. Hussein and M. Hamid. Scattering by a perfectly conducting cylinder with an axial infinite slot. In *Proc. Int. Symp. Recent Advan. Micr. Tech. ISRAMT91*, University of Nevada, Reno, NV, August 1991.

[16] A. kishk. Electromagnetic scattering from composite objects using a mixture of exact and impedance boundary conditions. *IEEE trans. Antennas Propagat.*, vol. AP-39, no. 6, pp. 826–833, June 1991.

[17] M. Hussein and M. Hamid. Scattering by a perfectly conducting multi-slotted cylinder. . *Cand. J. of Phys., In Press.*, 1992.

[18] C. P. Wu. Numerical solution for the coupling between waveguide in finite arrays. *Radio Sci.*, vol. 4, no. 3, pp. 245–254, March 1969.

[19] A-K. Hamid , I. R. Ciric and M. Hamid. Moment method solution of double step discontinuities in waveguides. *Int. J. Electronics*, vol. 65, no. 6, pp. 1159–1169, 1988.

[20] Roger F. Harrington. *Time-Harmonic Electromagnetic Fields.* McGraw Hill, New York, 1961.

[21] Roger F. Harrington. *Field Computation by Moment Methods.* Macmillan, New York, 1968.

[22] M.G. Andreasen. Scattering from parallel metallic cylinders with arbitarary cross section. *IEEE trans. Antennas Propagat.*, vol. AP-12, pp. 746–754, November 1964.